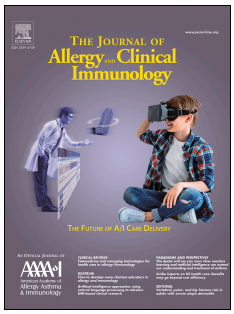
Journal Pre-proof



IL-4-BATF signaling directly modulates IL-9 producing mucosal mast cell (MMC9) function in experimental food allergy

Sunil Tomar, PhD, Varsha Ganesan, MSc, Ankit Sharma, PhD, Chang Zeng, PhD, Lisa Waggoner, BS, Andrew Smith, BS, Chang H. Kim, PhD, Paula Licona-Limón, PhD, Richard L. Reinhardt, PhD, Richard A. Flavell, PhD, Yui-Hsi Wang, PhD, Simon P. Hogan, PhD

PII: S0091-6749(20)31409-3

DOI: https://doi.org/10.1016/j.jaci.2020.08.043

Reference: YMAI 14789

To appear in: *Journal of Allergy and Clinical Immunology*

Received Date: 19 November 2019

Revised Date: 13 August 2020

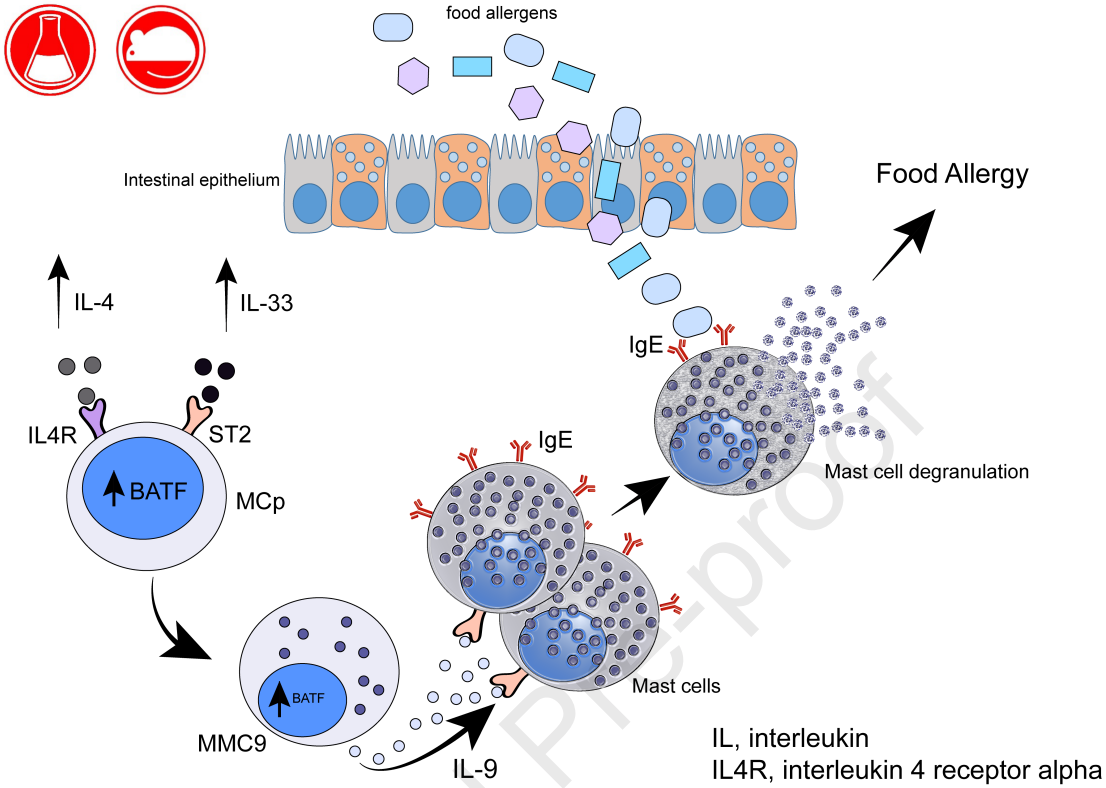
Accepted Date: 21 August 2020

Please cite this article as: Tomar S, Ganesan V, Sharma A, Zeng C, Waggoner L, Smith A, Kim CH, Licona-Limón P, Reinhardt RL, Flavell RA, Wang Y-H, Hogan SP, IL-4-BATF signaling directly modulates IL-9 producing mucosal mast cell (MMC9) function in experimental food allergy, *Journal of Allergy and Clinical Immunology* (2020), doi: https://doi.org/10.1016/j.jaci.2020.08.043.

This is a PDF file of an article that has undergone enhancements after acceptance, such as the addition of a cover page and metadata, and formatting for readability, but it is not yet the definitive version of record. This version will undergo additional copyediting, typesetting and review before it is published in its final form, but we are providing this version to give early visibility of the article. Please note that, during the production process, errors may be discovered which could affect the content, and all legal disclaimers that apply to the journal pertain.

© 2020 Published by Elsevier Inc. on behalf of the American Academy of Allergy, Asthma & Immunology.

IL-4-BATF signaling directly modulates IL-9 producing mucosal mast cell (MMC9) function in experimental food allergy



IL, interleukin
IL4R, interleukin 4 receptor alpha
ST2, IL-33 receptor,
MCp, mast cell progenitor

Journal Pre-proof

Journal Pre-proof

Title: IL-4-BATF signaling directly modulates IL-9 producing mucosal mast cell (MMC9) function in experimental food allergy

Running title: IL-4 signaling regulates MMC9 cells

Sunil Tomar, PhD,[a, b, c] Varsha Ganesan, MSc, [a, b, c] Ankit Sharma, PhD, [b, c] Chang Zeng, PhD,[a] Lisa Waggoner, BS,[a] Andrew Smith, BS,[a] Chang H. Kim, PhD,[b,c] Paula Licona-Limón, PhD,[d] Richard L. Reinhardt, PhD,[e,f] Richard A. Flavell, PhD,[d,g] Yui-Hsi Wang, PhD[a,h] and Simon P. Hogan, PhD[a,b,c]

[a]The Division of Allergy and Immunology, Cincinnati Children's Hospital Medical Center, Cincinnati, OH, US.

[b]Mary H Weiser Food Allergy Center, Michigan Medicine University of Michigan, Ann Arbor, MI, US

[c]Department of Pathology, Michigan Medicine, University of Michigan, Ann Arbor, MI, US

[d]Department of Immunobiology, Yale University School of Medicine, New Haven, Connecticut, USA.

[e]Department of Immunology and Microbiology, University of Colorado Anschutz Medical Campus, Aurora, CO, USA.

[f]Department of Biomedical Research, National Jewish Health, Denver, CO, USA

[g]Howard Hughes Medical Institute, Chevy Chase, Maryland, USA.

[h]Type 2 Inflammation and Fibrosis Cluster, Immunology & Inflammation Research, Sanofi, Cambridge, Massachusetts, USA

***Correspondence:** Simon P. Hogan, PhD, Mary H Weiser Food Allergy Center, Department of Pathology, University of Michigan 5063-BSRB 109 Zina Pitcher Place Ann Arbor, MI 48109-2200 Email: sihogan@med.umich.edu. Phone: 734-647-9923; Fax: 734-615-2331 and Yui-Hsi

Journal Pre-proof

Wang, PhD, Immunology and Inflammation Therapeutic Area, Sanofi Inc. 270 Albany St, Cambridge, MA 02139. Email: Yui-Hsi.Wang@sanofi.com.

Funding Sources: This work was supported by NIH DK073553, AI112626, AI138177, AI140133, DoD W81XWH-15-1-051730 (YH.W and S.P.H.) and Food Allergy Research & Education, M-FARA and Mary H. Weiser Food Allergy Center (S.P.H).

Abbreviations: MMC9, IL-9-producing mucosal mast cell; SI, small intestine; OVA, Ovalbumin; MCPT-1, Mast cell protease 1; MCP, mast cell progenitor; BM, bone marrow; MMC9-L, MMC9-like; LP, lamina propria; CAE, chloroacetate esterase; BATF, basic leucine zipper ATF-like transcription factor; scRNA-seq, single cell RNA sequencing

Conflicts of interest: The authors declare no conflicts.

Journal Pre-proof

Journal Pre-proof

Abstract

Background: We have previously identified IL-9 producing mucosal mast cell (MMC9) as the primary source of IL-9 to drive intestinal mastocytosis and experimental IgE-mediated food allergy. However, the molecular mechanisms that regulate the expansion of MMC9s remain unknown.

Objective: We hypothesized that IL-4 regulates MMC9 development and MMC9-dependent experimental IgE-mediated food allergy.

Methods: We utilized an epicutaneous sensitization-model and performed bone marrow (BM) reconstitution experiments, to test the requirement of IL-4Rα signaling on MMC9's in experimental IgE-mediated food allergy. Flow cytometric, bulk and single cell RNA-seq analysis on small intestine (SI)-MMC9s was performed to illuminate MMC9 transcriptional signature and the effect of IL-4Rα signaling on MMC9 function. BM-derived MMC9 culture system was used to define IL-4-BATF signaling in MMC9 development.

Results: Epicutaneous sensitization and BM reconstitution based models of IgE-mediated food allergy revealed an IL-4 signaling-dependent cell-intrinsic effect on SI- MMC9 cell accumulation and food allergy severity. RNA-seq analysis of SI-MMC9 cells identified 410 gene transcripts reciprocally regulated by IL-4 signaling, including *Il9* and Basic leucine zipper ATF-like transcription factor (*Batf*). *In silico* analyses identified a 3491-gene MMC9 transcriptional signature and identified two transcriptionally distinct SI-MMC9 populations enriched for metabolic or inflammatory programs. Employing an *in vitro* MMC9-culture model system we show that generation of MMC9-like cells was induced by IL-4 and this was in part dependent on BATF.

Conclusion: IL-4Rα signaling directly modulates MMC9 function and exacerbation of experimental IgE-mediated food allergic reactions. IL-4Rα regulation of MMC9s is in part BATF-dependent and via modulation of metabolic transcriptional programs.

Journal Pre-proof

Clinical Implications

Blockade of IL-4Rα-dependent pathways abrogate MC function and IgE-mediated food allergic responses through control of MMC9 cell functionality.

Key Words

Food allergy; Interleukin-4; Interleukin-9; mast cell; Basic leucine zipper ATF-like transcription factor; transcriptome, metabolism.

Journal Pre-proof

Journal Pre-proof

Capsule Summary

IL-4R/BATF-signaling mechanism regulates IL-9 producing mucosal mast cell transcriptional programs and induction of experimental IgE-mediated food allergy.

Journal Pre-proof

Journal Pre-proof

Introduction

Food allergies are an adverse IgE-mediated hypersensitivity reaction that affect millions of people worldwide (1, 2), with increasing prevalence over the past few decades (3, 4). Clinical symptoms of food allergy (FA) range from mild reactions to severe and affect multiple organs, including the gastrointestinal, respiratory, skin and cardiovascular systems (5). While recently an experimental biologic has been approved for peanut OIT treatment in allergic patients aged 4-17 years old, this therapeutic is to be used in conjunction with peanut-avoidant diet and has several limitations which prevent wider application (6). Thus, a better understanding of the immune mechanisms and signaling pathways underlying food allergy is clearly warranted to permit development of more effective and safe therapies to provide long term protection across patients of different ages and reactivity (7).

Over the last decade, there has been significant advancement in our understanding of the underlying basic mechanisms that drive IgE-mediated food-induced reactions. Experimental studies employing mouse model systems have identified a role for $CD4^+$ T helper 2 (Th2) cells and type-2 innate lymphoid cells (ILC2s) in the generation of food-specific IgE (8-10). Interleukin-4 (IL-4) induces IgE isotype switching and is required for food-specific IgE production by B cells and priming of the vascular endothelial compartment to mast cell-derived mediators including histamine (11-13). IL-9-IL9R signaling promotes MC maturation and induction of the necessary SI mastocytosis (14, 15). IL-13 stimulates intestinal epithelial secretory antigen passages (SAPs) that permits translocation of soluble dietary antigens directly to mucosal mast cells (MCs) leading to cross-linking the IgE bound to FcεRI on MCs and release of mediators, including histamine, platelet-activating factor, serotonin, proteases (tryptase and chymase) and lipid-derived mediators (prostaglandins [PGD2] and leukotrienes [LTC4, LTD4 and LTE4]), and induction of the clinical manifestations associated with food-triggered anaphylaxis (16, 17).

While there has been advancement in identification of the cellular source of IL-4 and IL-13 in food allergy, the cellular source of IL-9 is not fully illuminated (18). Our group previously identified a Lin^- c-Kit^+ FcεRIα^+ β_7-$integrin^{low}$ $ST2^+$ IL-9 producing cell population that secretes a prodigious amount of IL-9 and can rapidly develop into a granular MC following IL-3 + SCF exposure, which we have termed IL-9-producing mucosal mast cell (MMC9) (19). We have shown that the frequency of this population positively correlated with susceptibility to food allergy in different mice strains and adoptive transfer of MMC9s in sensitized mice led to the development of SI mastocytosis and rapid induction of food allergy symptoms (19). Collectively, these studies identify MMC9s as a critical cell that primes the intestinal environment for

induction of SI mastocytosis and subsequent development of food-induced IgE-mediated reactions (19). Importantly, the cytokine sequelae underlying the development and regulation of MMC9s, the existence of potential subpopulations and transcriptional programs expressed by MMC9 cells are largely unexplored.

In this study, we examined the role of IL-4 signaling in the regulation of MMC9 development and function, and in turn induction of food-induced anaphylaxis. Herein, we show that IL4 signaling directly regulates the accumulation of MMC9 in the SI and consequentially controls SI mastocytosis and anaphylaxis outcomes independent of effects on IgE and $CD4^+$ Th2 cells. Molecular analyses revealed that IL-4R-signaling regulates an MMC9 gene expression profile. Notably, loss and gain of function analyses revealed that IL-4R signaling directly regulates MMC9 expression of IL-9 and Basic leucine zipper ATF-like transcription factor (BATF). RNA-seq analysis identified a 3491-gene MMC9 transcriptional signature. scRNA-seq analysis of MMC9s identified transcriptionally distinct SI-MMC9 populations enriched for either metabolic or inflammatory programs. *In silico* approaches identified that the metabolic transcriptional program enriched in MMC9s was IL-4Rα-responsive. Utilizing, a novel MMC9-like cell culture model system and *Batf*$^{-/-}$ mice, we demonstrated that IL-4 promotes MMC9-like cell development in part via BATF-dependent process. Collectively, these studies identify an intricate role for IL-4R signaling in regulation of MMC9 transcriptional programs and functionality and exacerbation of food-induced anaphylaxis.

Journal Pre-proof

Methods:

Animals

Wild-type (WT) BALB/c, IL-4-IRES-eGFP (4GeT mice, stock number 004190) were originally provided by the Jackson Labs and bred in-house at Cincinnati Children's Hospital and Medical Center (CCHMC, Cincinnati, Ohio) and later at University of Michigan (Ann Arbor, Michigan). *Il4ra*$^{-/-}$ and *Il4ra*^{Y709F} mice were obtained from Fred Finkelman (CCHMC, Cincinnati, Ohio). IL-9-GFP (INFER mice) (20) were obtained from Richard Flavell (Yale University School of Medicine, New Haven, Connecticut). *Batf*$^{-/-}$ mice (21, 22) were provided by Richard L Reinhardt (National Jewish Health, Denver, Colorado). All the strains of mice used in these studies were on BALB/c background. All the experimental procedures were approved by the Institutional Animal Care and Use Committee of CCHMC and University of Michigan.

Adoptive transfer and epicutaneous sensitization based models of food allergy

For skin sensitization food allergy model, mice were first sensitized by applying 20 µl of MC903 (0.1 µM Calcipotriol, Tocris Bioscience, Bristol, UK), followed by 5µl of OVA (200mg/ml) (Sigma Aldrich, St. Louis, Missouri) to the ear for 14 days consecutively and then orally gavaged with OVA (50 mg in 250 µl saline) three times a week for a total of seven gavages (19). In reconstitution experiments, sensitized IL-4-GFP mice were intravenously injected with $5x10^6$ donor bone marrow cells one day after sub-lethal irradiation (9.5 Gy), then subjected to a second sensitization and seven oral OVA challenges, administered three times a week (14). Animals in mock sensitization groups were not sensitized with antigen for epicutaneous sensitization and adoptive transfer models of food allergy.

Measurement of parameters of food allergy

Mice were monitored for 45 minutes for food allergy symptoms after oral challenges. Mice were sacrificed 60 minutes after the last oral challenge. Hypothermia was measured by recording rectal temperature prior to last oral challenge and then again every 15 minutes after oral challenge for 45 minutes. Diarrhea incidence and hematocrit were recorded between 45-60 minutes after the last challenge as previously described (14). Blood samples and intestinal tissues were collected from mice immediately after mice sacrifice. Serum samples were analyzed using ELISA kits for OVA-specific IgE (MD Bioproducts, Oakdale, Minnesota), MCPT-1 (eBioscience, San Diego, California), and OVA-specific IgG1 (Alpha Diagnostic International, San Antonio, Texas). For intestinal histological analyses, duodenal tissues were fixed in 10% formalin and processed by standard histological techniques. 5 µm tissue sections were stained

with Leder stain for chloroacetate esterase (CAE) activity in intestinal mast cells (15). Stained cells were quantified as previously described (19).

Lamina Propria (LP) cell isolation

Small intestinal LP cell isolation was done as described previously (14). Briefly, small intestines were cut longitudinally and incubated in HBSS with 5 mM EDTA 4°C for 30 min before vortexing to remove epithelial cells. The remaining tissues were minced and digested with 2.4 mg/ml collagenase A (Roche Diagnostic, Indianapolis, Indiana) and 0.2 mg/ml DNase I (Roche) at 37°C for 30 min. After removal of tissue debris, liberated cells suspended in 44% Percoll were loaded above 67% Percoll before centrifugation. LP cells were collected from the interface between 44% and 67% Percoll, washed with complete media, and suspended in complete media.

Flow cytometric analysis and cell sorting

Viability of SI-LP cells was routinely confirmed > 95% using trypan blue exclusion. LP cells from small intestines of mice, treated with Fc Block (BD Biosciences, San Jose, California) were first stained with phycoerythrin (PE)-conjugated anti-c-Kit (2B8, BD Biosciences,), PE-Cy7-conjugated anti-FceRIα (MAR-1, Biolegend, San Diego, California), biotinylated anti-T1/ST2 (DJ8, MD Bioproducts, Oakdale, MN), allophycocyanin (APC)-conjugated anti-IL-17RB, APC-Cy7-conjugated anti-CD3e (145-2C11, BD Biosciences), V500-conjugated anti-CD4 (RM4-5, BD Biosciences), fluorescein isothiocyanate (FITC)-conjugated anti-β7integrin (M293, BD Biosciences), PerCP-Cy5.5-conjugated monoclonal antibodies against lineages (Lin) markers: CD11b (M1/70), CD11c (HL3), Gr-1 (RB6-8C5) (BD Biosciences), CD8α (53-6.7), B220 (RA3-6B2, Biolegend), followed by brilliant Violet 421-labeled streptavidin (Biolegend) before analysis with a FACSCanton II (BD Biosciences) or cell sorting with a FACSAria II (BD Bioscience). In some experiments, cells were prestained with Live/Dead NIR (Life technologies, Grand Island, NY) to confirm viability. MMC9 cells were identified by staining as SSC^{low} Lin- $CD3^{-}$ $CD4^{-}$ c-Kit^{+} $FceRI\alpha^{+}$ $ST2^{+}$ cells, $CD4^{+}$ Th2 cells were identified as SSC^{low} Lin^{-} $CD3^{+}$ $CD4^{+}$ IL17-RB^{+} cells similar to our previous study (23). ILC2s were identified as SSC^{low} Lin^{-} $CD3^{-}$ $CD4^{+}$ c-$Kit^{+/-}$ IL17-RB^{+} cells (10). BM-derived MMC9-L cells were identified by first staining with brilliant violet (BV) 421-conjugated anti-c-Kit (Biolegend), biotinylated anti-FceRIα (MAR-1, BD Biosciences), PE-Cy7-conjugated anti-ST2 (RMST2-2, Invitrogen, Carlsbad, California), BV786-conjugated anti-β7integrin (M293, Biolegend), APC-conjugated anti-CD27 (LG.7F9, Invitrogen), PerCP-Cy5.5-conjugated monoclonal antibodies against lineages (Lin) markers described above, including PerCP-Cy5.5-conjugated anti-CD3ε (BD Biosciences, San Jose, California), followed by APC-

Journal Pre-proof

Cy7-labeled streptavidin (BD Biosciences, San Jose, California). For intracellular staining of MMC9s, SI-LP cells were restimulated with Phorbol 12-myristate 13-acetate (PMA) (100ng/ml) and ionomycin (1µg/ml) and treated with golgi blocker (5ug/ml) (Sigma Aldrich), followed by fixation, permeabilization (Life Technologies) and staining with APC-anti-IL-9 (RM9A4, Biolegend) as described (19). For intracellular staining of MMC9-L cultures, cells were treated with golgi blocker (5µg/ml) in the last 5 hrs of the culture period and subsequently stained as described above.

MMC9-like culture model system

Bone marrow cells were obtained from Wild-type (WT) BALB/c, IL-9-GFP (20) and *Batf*$^{-/-}$ (21, 22) mice as previously described (24). Briefly, cells were cultured in complete media containing mSCF and mIL-3 (both 20 ng/ml) (Peprotech, Inc. Rocky Hill, New Jersey) for the first 6 days. On day 3, non-adherent cells were collected and resuspended in media containing mSCF and mIL-3. On day 6, non-adherent cells were obtained, spun down and suspended in media containing either SCF and IL-3 or the combination of mSCF, mIL-3 and mIL-4 (20ng/ml) (Peprotech, Inc. Rocky Hill, New Jersey). Cells were cultured for 4 more days, non-adherent cells were collected and suspended in media with fresh cytokines on d10 and resuspended at 1x 10^6 cells/ml, 200µl/well in 96 well plates. Cells were stimulated with mIL-33 (100ng/ml) for 24 hours.

Ex-vivo cytokine production and qPCR

For cytokine production, sorted MMC9s were washed with sterile flow cytometry buffer, resuspended in complete RPMI media and stimulated with PMA (100ng/ml) and ionomycin (1ug/ml) for 24 hours. Culture supernatants were used for IL-9 (Biolegend) and MCPT-1 ELISAs, as described previously. In some experiments, RNA lysates were prepared from sorted MMC9s for gene expression analysis by RNA-seq and qPCR.

Sequencing Analyses

Bulk RNA-seq sample preparation: RNA was isolated from freshly sorted MMC9s using the Quick RNA microprep kit (Zymo Research, California, USA). In some cases, cDNA synthesis was done using iScript reverse transcription supermix for RT-qPCR (Biorad). qPCR was performed for genes as described previously (19). In some experiments, RNA was used for RNA-seq performed using the Sequencing Core at CCHMC using pooled RNA samples from 12-20 biological replicates of mice for each group.

scRNA-seq sample preparation: Analyses was performed by CCHMC DNA Sequencing and Genotyping Core utilizing Fluidigm C1 Single Cell Full Length Messenger RNA (mRNA) Sequencing. In brief, single cell MMC9 cells (SI Lin-GFP^{hi} IL-17RB^{-} c-Kit^{+} ST2^{+} β7integrin^{low} cells) were prepared using the C1™ Single-Cell Auto Prep System (Fluidigm, San Fransisco, CA), according to the manufacturer's instructions. Flow-sorted cells were counted and suspended ~ 30,000 cells per 100 µl PBS and loaded onto a primed C1 Single-Cell Auto Prep Integrated Fluidic Chip for mRNA-Seq (5–10 µm). Cells were lysed on chip and reverse transcription was performed using Clontech SMARTer® Kit using the mRNA-Seq: RT + Amp (1771×) according to the manufacturer's instructions. Single cell cDNAs were transferred to a 96 well plate and diluted with 5 µl C1™ DNA Dilution Reagent and quantified using Quant-iT™ PicoGreen® dsDNA Assay Kit (Life Technologies, Grand Island, NY) and Agilent High Sensitivity DNA Kit (Agilent Technologies (Santa Clara, CA). Libraries were prepared using Nextera XT DNA Library Preparation Kit (Illumina Inc, Santa Clara, CA) on cDNAs at 100 pg/µl. In each single-cell library preparation, a total of 125pg cDNA was tagmented at 55 °C for 20 minutes. Libraries were pooled and purified on AMPure® bead-based magnetic separation before a final quality control using Qubit® dsDNA HS Assay Kit (Life Technologies) and Agilent High Sensitivity DNA Kit. We required the majority of cDNA fragments to be between 375–425bp to qualify for sequencing. Single cell libraries were subjected to paired-end 75bp RNA-Sequencing on a HiSeq 2500 (Illumina Inc., San Diego, CA). 96 scRNA-Seq libraries were sequenced per HiSeq 2500 gel (~300 million bp/gel).

RNA-seq Data processing

Bulk analyses: Raw reads were aligned to the reference mm9 mouse genome (GRCm38) using Hisat-build pipeline (25). Relative gene expression was quantified using FeatureCounts function from the subread-2.0.0 package (26). Differentially expressed genes were identified with at-least $\geq \pm 1.5$ fold Reads Per Kilobase of transcript, per Million mapped reads (RPKM) and heat map was generated using the Python on the normalized scale. PANTHER (27) and KEGG (28) databases were used to identify important pathways altered by differentially regulated genes within *Il4ra*^{Y709F}-MMC9, *Il4ra*$^{-/-}$-MMC9 and by the 410 genes reciprocally altered within both *Il4ra*^{Y709F}-MMC9 and *Il4ra*$^{-/-}$-MMC9. RNA-seq, as described in our previous study (14) was used to obtain correlational analysis between *Il9* and *Batf*/*Nfil3* mRNA expression.

Journal Pre-proof

To generate the 3491 gene transcript MMC9 transcriptome we identified common transcripts from the RNA-seq analyses of isolated WT MMC9 cells from the SI of food allergic mice (Supplementary Table S4) and 3738 gene transcripts described in GSE 72921 (19). Cell analyses of the MMC9 transcriptome was performed using the Enrichr tool (29, 30) and the BioGPS mouse cell type and Tissue gene expression profile Dataset (31-33) and protein-protein interaction network was identified using String (https://string-db.org/)(34). Functional and enrichment pathway analyses were performed using String (https://string-db.org/), DAVID (DAVID V6.8 (https://david.ncifcrf.gov/tools.jsp) (35, 36) and PANTHER V14.0 (http://pantherdb.org/) (37, 38) pathway enrichment databases.

Single cell RNA-seq analysis: We obtained scRNA-Seq reads from 81 SI Lin- IL-4GFP^{hi} IL-17RB^{-} c-Kit^{+} ST2^{+} β7integrin^{low} cells that were aligned to the reference mouse genome (GRCm38) to obtain relative gene expression as RPKM as described in the bulk sequencing analyses. n = 6 cells were excluded due to low quality cells as identified by low RPKM values and downregulated biological categories that correspond to basic molecular function and biological processes (results not shown). To exclude identification of gene transcripts that may be detected as part of random noise, we performed filtering analyses excluding transcripts that were detected in fewer than 15 % of the total cells (n = 75 cells). Prioritized transcripts based on average RPKM and expression by at least 10 cells. Functional and enrichment pathway analyses was performed on 10% DEGs (604 / 6030 genes) using DAVID (DAVID V6.8 (https://david.ncifcrf.gov/tools.jsp) (35, 36). We applied R Seurat package to identify the subpopulation of the MMC9 cells and Uniform Manifold Approximation and Projection (UMAP) (https://arxiv.org/abs/1802.03426)(39) dimensional reduction technique to visualize and explore these datasets. As a default, Seurat performs differential expression based on the non-parametric Wilcoxon rank sum test. We identified 3 subpopulations of MMC9 cells with this analysis. Differentially expressed genes with a ± 1.5 fold in IL-4 signaling from the bulk RNAseq of MMC9 cells were mapped over all the three clusters. Above 90% gene of the matched genes (between IL-4 signaling and scRNA-seq clusters) were mapped on metabolic cluster. Figure 5 represents the metabolic cluster mapped with IL4 signaling associated genes. Genes from this cluster were selected for gene-pathway network analysis. Functional and enrichment pathway analyses were performed using String (https://string-db.org/), DAVID (DAVID V6.8) (https://david.ncifcrf.gov/tools.jsp) (35, 36) and PANTHER V14.0 (http://pantherdb.org/) (37, 38) pathway enrichment databases. Input for pathway-gene interactions was prepared using Perl script, and the network was constructed and analyzed using Cytoscape 3.7.1 (40).

Journal Pre-proof

Statistical analysis. In experiments comparing multiple experimental groups, statistical differences between groups were analyzed using the one/two-way ANOVA parametric test. In experiments comparing two experimental groups, statistical differences between groups were determined using a Student's t-test or Wilcoxon-Mann-Whitney test. Results are considered significant at $P \leq 0.05$. All data was analyzed using Prism (GraphPad Software, San Diego, CA, USA).

Journal Pre-proof

Results:

IL-4 signaling drives SI MMC9 to control food allergic outcomes.

To gain insight into the impact of IL-4 signaling on MMC9s in the food allergic phenotype in mice, we employed complementary IL-4Rα gain and loss of function approaches utilizing wild type (WT), *Il4ra*^{Y709F} (41) and *Il4ra*$^{-/-}$ mice (42). Epicutaneous sensitization and repeated oral gavage challenge with Ovalbumin (OVA) antigen (Figure S1A) (19) increased the SI Lamina propria (SI-LP) frequency and total numbers of Lin^{-} c-Kit^{+} FcεRIα^{+} ST2^{+} IL9^{+} MMC9s and CD4^{+} IL-17RB^{+} Th2 cells in WT mice (Figure 1A-E, Figure S1B and S2A) (19). Genetic deletion of *Il4ra* abrogated OVA-induced amplification of SI MMC9 and CD4^{+} Th2 cells (Figure 1 A-E and Figure S2A). Conversely, gain of function of the *Il4ra* (*Il4ra*^{Y709F} mice) led to increased percentage and total numbers of SI MMC9 cells and CD4^{+} Th2 cells compared to WT mice (Figure 1A-E and Figure S2A). Percentage and total numbers of SI Lin^{-} CD3^{-} CD4^{-} IL-17RB^{+} ILC2s in *Il4ra*^{Y709F} mice were significantly reduced compared to the WT mice and *Il4ra*$^{-/-}$ mice (Figure 1F and Figure S2A and B). Importantly, the opposing effects of IL4Rα-signaling on SI MMC9 and CD4^{+} Th2 cell levels in *Il4ra*$^{-/-}$ and *Il4ra*^{Y709F} mice were directly associated with development of IgE-mediated food allergy (Figure 1G-L). Moreover, *Il4ra*$^{-/-}$ *mice* that possessed reduced levels of SI MMC9 and CD4^{+} Th2 cells compared with WT mice, did not develop symptoms of food allergy (diarrhea and hypovolemic shock) or demonstrate an SI mastocytosis or systemic MC activation (Figure 1G-L). Conversely, *Il4ra*^{Y709F} mice which demonstrated heightened levels of SI MMC9 and CD4^{+} Th2 cells compared with WT mice, demonstrated a more severe food allergy phenotype (diarrhea and hypovolemic shock) and possessed exaggerated SI mastcocytosis and systemic MC activation (Figure 1G-L). The increased incidence and severity of food-induced anaphylaxis in *Il4ra*^{Y709F} mice was not related to increased serum levels of OVA-specific IgE or MMC9 FcεRIα expression, however total serum IgE levels were significantly increased in *Il4ra*^{Y709F} mice (Figure S2C-E). Furthermore, demonstration that MMC9 levels in mock-sensitized *Il4ra*^{Y709F} mice following repetitive oral OVA gavage challenge was significantly lower than that observed in epicutaneously sensitized and repeated oral gavage challenged *Il4ra*^{Y709F} mice and comparable to that observed in sensitized and challenged *Il4ra*$^{-/-}$ mice indicates that the observed heightened SI MMC9 levels is not a

consequence of increased basal levels (Figure S3A). We concluded that IL-4 signaling impacts antigen-induced $CD4^+$ Th2 cell and MMC9 frequency and function and development of food-induced anaphylaxis.

IL-4 signaling in MMC9 cells is required for food-induced SI MMC9 amplification and food allergic responses.

To determine if IL4Rα signaling directly impacted MMC9 function, we employed an adoptive transfer model of food allergy (19) whereby OVA-sensitized WT mice are sub-lethally irradiated and reconstituted with bone marrow (BM) from WT, *Il4ra*^{Y709F} or *Il4ra*$^{-/-}$ mice and subsequently receive repeated oral challenges (Figure S4A-B). The advantage of this model system is that it permits distinction between the requirement of IL-4Rα on $CD4^+$ T cells and MMC9 cells as recipient mice possess $CD4^+$ Th2 cells of recipient origin and innate cells including MMC9s and ILC2s, from donor origin (Figure S4C and D) (19). Transfer of WT BM to OVA-sensitized WT mice and repeated oral challenge with OVA reconstituted the SI $CD4^+$ Th2 compartment and maintained the levels of ILC2 and MMC9 cells to levels comparable to that observed in WT mice sensitized and repetitively challenged with OVA (Figure 1C-F and 2A and B). OVA challenge of WT mice reconstituted with *Il4ra*^{Y709F} BM induced significantly higher frequency of MMC9s compared to WT mice that received WT BM (Figure 2A and B) and conversely, OVA challenge of WT mice that received *Il4ra*$^{-/-}$ BM had significantly lower frequency of MMC9s (Figure 2A and B). Consistent with previous observations, SI LP-sorted MMC9s derived from WT, *Il4ra*^{Y709F} or *Il4ra*$^{-/-}$ origin possessed a hypogranular phenotype (Figure S5) (19). The frequency of $CD4^+$ Th2 cells and ILC2s was similar between groups suggesting that IL-4 signaling directly regulates the expansion of MMC9 cells independent of $CD4^+$ Th2 cells (Figure 2A and B). Importantly, the reciprocal regulation of the levels of SI MMC9 cells was associated with the development of SI MCs, systemic MC activation and development of the food allergy phenotype (Figure 2C-F and S6). That is, WT mice that received *Il4ra*^{Y709F} BM possessed heightened SI MCs, systemic MC activation and disease symptoms (diarrhea occurrence) following dietary antigen challenge compared to mice that received WT BM. Conversely, WT mice that received *Il4ra*$^{-/-}$ BM did not develop SI mastocytosis or have evidence of systemic MC activation or disease symptoms following OVA challenge (Figure 2 C-F and S6A). Importantly, the altered SI MMC9 cells and MC phenotype was not related to changes in OVA-specific or total IgE (Figure 2F and S6B). Furthermore, repetitive oral OVA gavage challenge of mock-sensitized WT mice that received *Il4ra*^{Y709F} BM did not amplify SI MMC9 levels indicating that the observed phenotype is not a consequence of heightened basal levels of *Il4ra*^{Y709F} SI MMC9 levels (Figure S3B).Next, to

determine whether the effect of IL-4 signaling on MMC9 was associated with altered IL-9 production, we compared the *Il9* gene and protein expression of flow-sorted MMC9 cells of WT, *Il4ra*^{Y709F} and *Il4ra*$^{-/-}$ origin from SI-LP of recipient WT mice. *Il9* mRNA and protein expression was increased ~2-3 fold in *Il4ra*^{Y709F}-derived MMC9 as compared to WT-derived MMC9 cells (Fig 2G). These datasets suggest a role for IL-4Rα signaling in IL-9 expression in MMC9 cells and MMC9 frequency and control of food allergen-induced SI mast cell levels, MC activation and concomitant food allergic outcomes.

IL-4 signaling directly regulates MMC9 gene expression

To gain greater insight into the IL4Rα-dependent regulation of MMC9 function we performed RNA-sequencing analysis of flow-sorted MMC9s from SI-LP of WT mice reconstituted with MMC9s of WT, *Il4ra*^{Y709F} and *Il4ra*$^{-/-}$ origin. We identified dysregulation of 4253 genes (n = 2437*Il4ra*^{Y709F}, n = 2957 *Il4ra*$^{-/-}$, FC > ± 1.5-fold) in *Il4ra*^{Y709F} and *Il4ra*$^{-/-}$-MMC9s compared with WT MMC9 cells (Figure 3A). 2437 genes (Up n = 981, Down n = 1456, FC > ± 1.5-fold) were significantly altered in expression in *Il4ra*^{Y709F} MMC9s (Figure 3A and Supplementary Table S1) and 2,957 genes (Up n = 1874, Down n = 1083, FC > ± 1.5-fold) were significantly altered in expression in *Il4ra*$^{-/-}$ MMC9s (Figure 3A and Supplementary Table S2). Of the 42C53 dysregulated genes, 1141 genes were dysregulated in both *Il4ra*^{Y709F} and *Il4ra*$^{-/-}$ MMC9 cells and 410 of these genes were reciprocally dysregulated in both *Il4ra*^{Y709F} and *Il4ra*$^{-/-}$ MMC9 cells compared with WT (Figure 3A-C and Supplementary Table S3). Moreover, 102 genes were increased in *Il4ra*^{Y709F} and decreased in *Il4ra*$^{-/-}$ MMC9 cells; and 308 genes were decreased in *Il4ra*^{Y709F} and increased in *Il4ra*$^{-/-}$ MMC9 cells (Figure 3A-C). Within these 410 reciprocally-regulated genes (Figure 3B), *Il9* was identified as the most dysregulated gene, with 5.2-fold induction in *Il4ra*^{Y709F} MMC9s and 7-fold reduction in *Il4ra*$^{-/-}$ MMC9s (Figure 3B and C). Notably, we also observed reciprocal dysregulation of two transcription factor genes by IL-4 signaling: Basic leucine zipper ATF-like transcription factor (BATF) and NFIL3, encoded by the gene E4 promoter-binding protein 4 (E4bp4) (Figure 3B-D). Indeed, correlation analyses of mRNA levels of *Il9* and *Batf* across multiple cell types, including MMC9s, ILC2s, Th2, BM-derived MCs, peritoneal MCs, mast cell progenitors (MCp), $CD8^+$ T cells, eosinophils, B cells, and non-Th2 CD4 T cells revealed a strong positive correlation between *Il9* and *Batf* expression (Figure 3E and F). These studies reveal that IL-4Rα signaling regulates IL-9 mRNA expression in MMC9s and expression of this cytokine correlated with *Batf* and *Nfil3* mRNA expression.

MMC9 Transcriptome

We have previously performed RNA-seq analyses on isolated MMC9 cells from the SI of food allergic mice and identified 3738 gene transcripts (GSE 72921) (19). Herein, we identified 9,408 expressed genes in WT-origin MMC9 cells purified from the SI of food allergic WT recipient mice that received WT BM (Supplementary Table S4). Comparison of the two gene expression profiles identified 3491 common gene transcripts, which we now define as the MMC9 transcriptional signature (Figure 3G and Supplementary Table S5). Analyses of the MMC9 transcriptome revealed that the differentially expressed genes (DEGs) were significantly enriched for many canonical mast cell proteases, mast cell protease (*Mcpt*) *Mcpt1, Mcpt2, Mcpt4, Mcpt8, carboxypeptidase A3 (Cpa3), chymase (Cma) -1 and 2, cathepsin G (Ctsg)* as well as mast cell-specific genes: *Fc Fragment Of IgE Receptor Ia* (*Fcer1a)*, *ADAM Metallopeptidase With Thrombospondin Type 1 Motif 9* (*Adamts9*), *Hematopoietic Prostaglandin D Synthase (Hpgds), L-tryptophan transporter (Slc7a5), DOPA decarboxylase (Ddc) monoamine oxidase (Maob)* (Supplementary Table S6) (43). DAVID functional annotation clustering analyses of the 3491 common DEGs identified enrichment of GO molecular functions involved in the regulation of transcriptional activity (RNA and mRNA binding), cell-cell adhesion (cadherin binding) and intracellular signaling (Ubiquitin, kinase and purine ribonucleoside binding) and biological processes including gene expression, rRNA processing and metabolic processes (Supplementary Table S6). KEGG pathway enrichment analyses revealed highly significant enrichment in DEGs associated with disease-related dysfunctional and metabolic disorders (Alzheimer's disease, Parkinson's disease, Huntington Disease and NAFLD) and metabolic pathways (thermogenesis, oxidative phosphorylation) (Figure 3H; Supplementary Table S6)

scRNA-seq analyses MMC9 cells

To analyze potential transitional intermediates or subsets of MMC9 cells, we performed single-cell RNA sequencing (scRNA-seq) on n = 81 purified SI Lin-GFP^{hi} IL-17RB^{-} c-Kit^{+} ST2^{+} β7integrin^{low} cells from WT food allergic mice (Figure 4A). Prioritization of transcripts based on average RPKM and expression by at least 10 cells revealed the top 50 expressed transcripts in n = 75 cells (Figure 4A) to be genes related to mast cell function: *Cpa3*, *Mcpt1*, *Hdc*, *Tph1*, *Srgn*, *Fcer1a*, *Cma1*, *Tpsb2*, *Gzmb*, *Mcpt2*, *Kit*, *Ms4a2*, *Mcpt4*, *Gata2*, *Rac2*, *Cd63*, *Alox5*, *Ccl2* (Figure 4B). Overall, we identified expression of a total of 6030 genes in n = 75 cells (Supplementary Table S7). Employing a supervised cell type mapping approach, n = 75 cells expressed at least 3100 of 3491 transcripts of the MMC9 transcriptional signature (Supplementary Table S5 and S7). Furthermore, DAVID pathway analyses of the top 10%

DEGs (604 / 6030 genes) revealed significant enrichment for mast cell genes and transcripts that regulate mRNA splicing and transcriptional activity, protein phosphorylation (ATP-binding and transferase activity), mast cell activity (positive regulation of mast cell degranulation and IgE receptor activity) and protein processing (serine-type endopeptidase activity) confirming that these cells are mast cell lineage (Supplementary Table S8). n = 6 cells were not included in the analyses due to low quality cells as identified by downregulated biological categories that correspond to basic molecular function and biological processes (results not shown). Gene expression clustering using Seurat Uniform Manifold Approximation and Projection (UMAP) dimensional reduction technique partitioned the n = 75 MMC9 cells into three distinct clusters (n = 71 total MMC9 cells: Cluster 0 (n = 30 cells) (metabolic), 1 (n = 24 cells) (inflammatory) and 2 (n = 17 cells) (other)) (Figure 4C and D). Cluster 0 was enriched for n = 370 gene transcripts of the MMC9 transcriptional signature and pathway enrichment analyses (DAVID and PANTHER pathway-classification system) revealed enrichment for transcripts that encoded for products in the categories of metabolism including cellular metabolic process, metabolism of proteins, thermogenesis, metabolic pathways, Non-alcoholic fatty liver disease (NAFLD) and mitophagy relative to the abundance of transcripts encoding products in other pathways (Supplementary Table S9 and S10). Cluster 1 “inflammatory” MMC9 population was enriched for 19 MMC9 signature transcripts and pathways involved in inflammation including Toll-like receptor signaling pathway, JAK-STAT signaling pathway, Cytokine-cytokine receptor interaction) pathways (Supplementary Table S9 and S10) Cluster 2 was enriched for n = 5 MMC9 genes that were not determined to be significantly enriched in any functional category or pathway (Supplementary Table S9 and S10). Based upon these analyses we concluded that within the SI of food allergic mice there are at least n = 2 MMC9 populations defined by transcriptional signature that can be categorized into metabolic and inflammatory MMC9 cells. To gain insight into which MMC9 population is responsive to IL-4 signaling, we mapped the IL-4R responsive genes identified by analysis of the dysregulated genes (*Il4ra*^{Y709F} versus WT MMC9 RPKM > 5, *Il4ra*^{Y709F} > 0; ± 1.5-fold; n = 2437 genes) and (*Il4ra*$^{-/-}$ versus WT MMC9 RPKM WT > 5, *Il4ra*$^{-/-}$ > 0; ± 1.5-fold; n = 2,957 genes) (Supplementary Table S1 and S2) to the metabolic, inflammatory and other MMC9 populations. 106 genes mapped to the MMC9 populations of which 100 genes mapped to Cluster 0 metabolic population, n = 4 genes to the inflammatory MMC9 cells and n = 2 genes to other MMC9 population (Supplementary Table S11). Notably, IL-4 signaling responsive genes in MMC9 cells that mapped to the metabolic population were significantly enriched for genes encoding for products in the functional pathways of metabolism (2-oxoglutarate

metabolic, cellular nitrogen compound metabolic, cellular aromatic compound metabolic) suggesting that IL-4-IL-4Rα-signaling modulates the metabolic MMC9 cell subset (Figure 5).

IL-4 signaling induces *in vitro* development of BM-derived MMC9-like cells

To directly test the role of IL-4R-signaling in regulation of MMC9 development and maintenance, we established an *in vitro* model system to generate MMC9-Like (MMC9-L) cells from BM progenitors derived from IL-9-GFP mice (Figure 6A). The IL-9 reporter knock-in mice designated INFER (Interleukin Nine Fluorescent Reporter) permits identification of IL-9 expressing cells in real time (20). We have previously demonstrated that ex vivo MMC9 cells are Lin$^-$ c-Kit$^+$, FcεRIα$^+$, ST2$^+$, Thy1.2$^+$, MHCII$^+$, CD86$^+$, IL-2Rα$^-$, IL-7Rα$^-$, Sca-1$^-$, CD23$^-$, CCR3$^-$, Siglec-F$^-$, or IL-3Rα (CD123)$^-$ indicating that this cell is of the MC lineage (19, 44) and, that these cells rapidly lose their IL-9-producing capability and develop into mature MCs following IL-3 + SCF culture (19). We therefore cultured whole BM in the presence of IL-3 + SCF until we observed appreciable numbers of MC progenitors (Lin$^-$ c-Kit$^+$ FcεRIα^{high} β_7-integrin^{high} ST2$^+$) in the absence of mature MCs, and subsequently exposed the cells to the cytokine IL-4 and subsequently IL-4 + IL-33 which is a known trigger of IL-9 production (19). On Day 0, MC progenitors (Lin$^-$ c-Kit$^+$ FcεRIα^{high} β_7-integrin^{high} ST2$^+$) were undetectable (Figure S7A top row; Black and purple boxes). Exposure of whole BM to SCF + IL-3 for six days generated significant numbers of MC progenitors (Lin$^-$ c-Kit$^+$ FcεRIα^{high} β_7-integrin^{high} ST2$^+$) in the absence of mature MCs (Figure S7A bottom row; black and purple boxes). A Lin$^-$ c-Kit$^+$ FcεRIα^{mid} β_7-integrin^{low} ST2$^-$ population was detected in whole BM on Day 0 (Figure S7A top row; Blue and orange boxes) and increased three-fold following six days of SCF + IL-3 exposure (Figure S7A bottom row; Blue and orange boxes) that appeared to represent an early MC lineage population. In the absence of SCF + IL-3 we did not observe MC lineage commitment or presence of mature MCs (Lin$^-$ c-Kit$^+$ FcεRIα^{high} β_7-integrin^{low} ST2$^+$ IL-9-GFP$^-$) cells (results not shown). Next we exposed Day 6 BMMC cultures to SCF + IL-3 + IL-4 for 96 hours followed by IL-33 for twenty-four hours and examined for IL-9-GFP expression (Figure 6A). Stimulation of BM cells with SCF + IL-3 for ten days followed by twenty-four hours of IL-33 predominantly lead to the generation of mature MCs (Lin$^-$ c-Kit$^+$ FcεRIα^{high} β_7-integrin^{low} ST2$^+$ IL-9-GFP$^-$) cells (Figure 6B Top row; grey and black Boxes). We also observed the presence of c-kit$^+$ FcεRI$^{low/mid}$ β7-integrin^{high} ST2$^+$ cells that were predominantly IL-9-GFP$^-$ (Figure 6B Top row; blue and green populations). Culturing of BM cells with IL-3 + SCF + IL-4 for 4 days and twenty-four hours of IL-33 predominantly lead to the generation of mature MCs (Lin$^-$ c-Kit$^+$ FcεRIα^{high} β_7-integrin^{low} ST2$^+$

IL-9-GFP$^-$) cells (Figure 6B bottom row; grey Box and black boxes). However, we also observed the potent induction of IL-9 within Lin$^-$ c-Kit$^+$ FcεRIα$^{low/mid}$ β_7-integrin^{low} ST2$^+$ cells upon IL-33 stimulation (Fig 6B bottom row Blue and green boxes and Fig 6C). qRT-PCR analyses revealed that purified Lin$^-$ c-Kit$^+$ FcεRIα$^{low/mid}$ β_7 Integrin^{lo} ST2$^+$ cells expressed *Il9, Nfil3* and *Batf* mRNA supporting the notion that this population is similar to the observed ex vivo MMC9 cells (Supplementary Figure S8). Thus, we defined this Lin$^-$ c-Kit$^+$ FcεRIα$^{low/mid}$ β_7 Integrin^{low} ST2$^+$ population as "MMC9-like cells" (MMC9-L cells) because of similarity to the *in vivo*-defined Lin$^-$ c-Kit$^+$ FcεRIα$^+$ ST2$^+$ β_7^{low} MMC9 cells. Comparison of Lin$^-$ c-Kit$^+$ FcεRIα$^{low/mid}$ ST2$^+$ and mature BM-derived MCs (c-Kit$^+$ FcεRIα^{high} ST2$^+$ cells) revealed that IL-9 was restricted to MMC9 cells (Figure 6B, C), and required IL-33 (Figure 6C). Taken together, our results suggest that IL-4 has the capacity to directly induce IL-9 expression in Lin$^-$ c-Kit$^+$ FcεRIα$^{low/mid}$ β7-integrin^{low} ST2$^+$ MMC9-like cells *in vitro*.

Given our demonstration that *Batf* expression in SI-MMC9s was responsive to IL-4 signaling (Figure 3A-D), and that *Il9* mRNA expression positively correlated with *Batf* mRNA across different cell types (Figure 3E), we were next interested in defining the requirement of the BATF in IL-4-induced MMC9-L cell development. WT (BALB/c) and *Batf*$^{-/-}$ BM cells were cultured under MMC9-like conditions (Figure 6A) and following twenty-four hours of IL-33 exposure IL-9 expression was examined. We show that loss of BATF signaling lead to a significant reduction (~50%) in MMC9-like cell formation (Lin$^-$ c-Kit$^+$ FcεRIα$^{low/mid}$ β_7-integrin^{low} ST2$^+$ IL9$^+$) cells (Figure 6D and E). Notably, we observed no reduction in mature MCs (Lin$^-$ c-Kit$^+$ FcεRIα$^+$ β_7-integrin^{low} ST2$^+$ IL-9$^-$) cell frequency between groups (Figure S7B). Collectively these studies show that IL-4-induced MMC9 development is in part dependent on BATF.

Discussion:

We previously identified a Lin$^-$ c-Kit$^+$ FcεRIα$^+$ β_7-integrin^{low} ST2$^+$ IL-9-producing cell population that secretes a prodigious amount of IL-9, induce intestinal mastocytosis, rapidly develops into a granular MC following IL-3 + SCF exposure and drive symptoms of food-induced anaphylaxis (19). Here in, employing *Il4ra*^{Y709F} and *Il4ra*$^{-/-}$ mice and a reconstitution model of food allergy, we identified an IL-4Rα signaling-dependent regulation of MMC9 cell amplification in food allergy that was independent of IL-4Rα-signaling involvement in Th2 cell function or antigen specific-IgE responses. RNA-seq analysis of SI MMC9 cells identified an IL-4Rα-regulated MMC9 transcriptome that includes IL-9, BATF and NFIL3. ScRNA-seq analyses revealed two transcriptionally distinct MMC9 populations enriched for metabolic or inflammatory

578 programs. IL-4 responsive genes were predominantly restricted to the metabolic networks
579 suggesting that IL-4 signaling may regulate MMC9 metabolic programming. Employing a novel
580 *in vitro* MMC9 culture system, we show that IL-4 significantly increased MMC9-L cells (Lin^- $c\text{-}Kit^+$
581 $Fc\varepsilon RI\alpha^{low/mid}$ β_7-$integrin^+$ $ST2^+$ IL-9-GFP^+) *in vitro*. Finally, using *Batf*$^{-/-}$ mice we showed that IL-4
582 mediated induction of MMC9-L cells was in part regulated by BATF. Based upon these studies
583 we conclude that direct IL-4Rα signaling can enhance MMC9 cell development and function
584 which in turn regulates SI mastocytosis and IgE-mediated food allergic response.

585 The initial identification of IL-4 from a mouse helper T cell cDNA library describes a 140
586 amino acid secreted protein that possessed B-cell, T-cell and mast cell proliferative capacity
587 (45). Subsequent follow-up studies revealed that IL-4 alone possessed minimal capacity to
588 promote MC proliferation (46); however IL-4 could amplify IL-3-dependent MC growth (47, 48)
589 and support clonal proliferation of connective tissue MCs (49). Since these initial descriptions,
590 IL-4 has been shown to possess multiple positive and negative regulatory effects on MC
591 maturation and function (50, 51). IL-4 prolongs mast cell survival, stimulates mediator release
592 (52, 53) and adhesion molecule expression (ICAM-1 and LFA-1) (54, 55). Whereas, IL-4 inhibits
593 murine MC FcεRI (56) and mucosal mast cell protease (MCPT-1, MCPT-2) expression (57).
594 While these studies suggest that IL-4 can directly impact MC growth, our studies reveal an
595 indirect mechanism by which IL-4 can modulate MC frequency and function via regulation of the
596 MMC9 population which is a critical requirement for dietary antigen-induced SI mastocytosis
597 and food-induced anaphylaxis (19).

598 Herein, we reveal a requirement for IL-4Rα signaling directly on MMC9 cells for the
599 amplification of SI MMC9 frequency and subsequent development of SI mastocytosis in food-
600 induced anaphylaxis. Moreover, contracted SI MMC9 levels in the presence of normal levels of
601 allergen specific IgE, $CD4^+$ Th_2 cells and ILC2 cells protected against food-induced anaphylaxis,
602 Conversely, heightened SI MMC9 levels was sufficient to exacerbate food-induced anaphylaxis.
603 The primary role for MMC9 cells appears to relate IL-9 induction to SI mastocytosis during
604 dietary antigen exposure (19). We have previously reported a critical role for IL-9 / IL-9R
605 signaling in the induction of SI mastocytosis and development of food-induced anaphylaxis (14).
606 Furthermore, we have shown that overexpression of IL-9 in the SI is sufficient to induce SI
607 mastocytosis (23). IL-9 is not sufficient to induce MC growth and differentiation of MCps, but can
608 enhance SCF-dependent MC growth (58). Employing *Il4ra*^{Y709F} *mice,* Burton and colleagues
609 have previously reported a cell intrinsic effect of IL-4 on intestinal MC homeostasis (59). The
610 authors showed that IL-4 is sufficient to drive intestinal mastocytosis (59) and that IL-4

enhanced MC growth and survival was through the induction of anti-apoptotic genes Bcl-2 and Bcl-X_L. In concordance with our studies, the authors revealed that IL4Rα-signaling directly promoted MC expansion during food allergy in mice (59). Intriguingly, Burton and colleagues identified SI mast cells as Lin$^-$ CD45$^+$ c-kit$^+$ IgE$^+$ cells (59). Notably, we show that during a food allergic reaction, both the SI mature MCs and MMC9 cells are Lin$^-$ c-kit$^+$ FcεRIα$^+$ and can only be distinguished by expression of IL-9 and side scatter characteristic (SSC). Burton et al., did not distinguish whether the IL-4-induced increase in MC populations was restricted to mature MC's or also due to an increase in MMC9 level. Our studies employing *Il4ra*$^{-/-}$ and *Il4ra*^{Y709F} global mice reveal that IL4Ra signaling directly impacts both MMC9 and mature MC frequency, however if you restrict IL4Ra signaling on MMC9 population you can impact total mature MC frequency suggesting that IL-4Rα-dependent effects are via regulation of MMC9 cells.

In the adult mouse, BM multipotential progenitor (Lin$^-$ CD27$^-$ FcεRIα$^-$ β_7-integrin$^+$) cells give rise to splenic basophil mast cell progenitors (BMCP- Lin$^-$ c-kit$^+$ FcγRII/III$^+$ β_7-integrin^{hi} FcεRI$^-$) and committed mast cell progenitors (MCp- Lin$^-$ CD45$^+$ CD34$^+$ c-kit$^+$ β_7-integrin^{hi} FcεRIα$^+$) (60-62) that are considered to serve as MC-committed progenitors that populate tissues with mature MCs (61, 63, 64). In particularly, MCps have been shown to be recruited to the GI tract via β_7-integrin- and CXCR2-dependent mechanisms and are required for maintenance of mature MC population (65). Our *in vitro* data suggests that IL-4 + SCF/IL-3 exposure of BM progenitors leads to the generation of MMC9-like cells. It is currently unclear what specific MCp subset leads to MMC9 commitment or the temporal and spatial conditioning signals required for the commitment to MMC9 cells. Importantly, IL-4 alone was not sufficient to permit visualization of the IL-9-GFP signal or IL-9 secretion. The cells required additional signals such as IL-33 to visualize IL-9-GFP and IL-9 secretion. Previous studies have reported IL-33-induction of IL-9 in both human CD4$^+$ T cells and basophils (66). IL-4 was required for IL-33-driven induction of IL-9 in MMC9 cells as we observed a very low frequency of MMC9 cells following IL-33 stimulation alone. The requirement of IL-4 was not related to level of expression of IL-33R, as we did not observe differential expression of the IL-33R, ST2 in *Il4ra*^{Y709F} and *Il4ra*$^{-/-}$ Lin$^-$ c-Kit$^+$ FcεRIα$^+$ IL9$^+$ MMC9 gene expression profiling analyses and previous reports indicate high ST2 expression on MCps. Importantly, in accordance with our previous studies, IL-9 was restricted to hypogranular Lin$^-$ c-Kit$^+$ FcεRIα$^+$ ST2$^+$ cells and that highly granular mature Lin$^-$ c-Kit$^+$ FceRIα$^+$ ST2$^+$ MCs were IL-9 negative (19). Consistent with this, previous studies have reported that MCs derived from BM progenitors stimulated with IL-4 and SCF possessed a hypogranular phenotype (46).

643 Gene expression profile analysis identified a IL-4Rα-regulated MMC9 transcriptome that
644 included the transcription factors BATF and NFIL3. Previous studies have reported a role for
645 BATF and IRF4 in IL-33-ST2-dependent FoxP3^{+} regulatory T cell development and
646 maintenance (67). Notably examination of the MMC9 transcriptome from *Il4ra*^{Y709F}- MMC9 cells
647 identified significant induction of IRF4 highlighting the possibility of a role for BATF and IRF4 in
648 IL-33 induction of IL-9. A large transcriptional network involving the canonical Th2-promoting
649 transcription factors, GATA-3 and STAT6, the ETS family transcription factor, (PU.1, IRF4),
650 BATF and BATF3, have been shown to bind to conserved regulatory elements at the *Il9* locus
651 (CNS2 / CNS +5.5; CNS0/CNS-6; CNS-12; CNS-25 and CNS-35), thereby stabilizing IL-9
652 expression and supporting Th9 cell differentiation (68-71). Analyses with *Batf*$^{-/-}$ BM cells
653 revealed a role for BATF in the IL-4-induction of MMC9 cells. IL-4-STAT6 signaling in Th9 cells
654 promotes BATF expression (68) and IL-4 can modulate BATF functionality through an IL-
655 4/BATF/IRF4 positive feedback amplification loop (72). Recently, investigators demonstrated
656 that the CNS25 region of the *Il9* promoter which binds to several TFs including IRF4, SMAD2/3
657 and BATF is required for *Il9* transcription in mature MCs (70). Deletion of this region in mice
658 lead to decreased SI MCs and diminished food allergy suggesting that the CNS-25 region of *Il9*
659 promoter is required for IL-9 expression in mast cell populations (70). The demonstration that IL-
660 4 can induce MMC9-L cells from *Batf*$^{-/-}$ BM indicates that BATF is not essential for MMC9-L
661 development. Previous studies have reported functional redundancy amongst BATF family
662 members (BATF, BATF2 and BATF3) likely via the common activity of their leucine zipper
663 domains and BATF3 expression is sufficient to promote Th9 cell development in the absence of
664 BATF (73, 74). Whether BATF is required for *Il9* gene expression or plays a more integral role in
665 MMC9 fate decisions is currently unknown. The other TF that was reciprocally regulated during
666 exaggerated and loss of IL-4Rα function was NIFL3. NFIL3, encoded by the gene E4 promoter-
667 binding protein 4 (*E4bp4*) is a basic leucine zipper transcription factor that regulates *Il3*
668 promoter activity in immune cells (75, 76). NFIL3 is required for the development of Peyer's
669 patches and establishment of ILC subsets into GI tract (77) and CD4^{+} Th2 responses (78). IL-4
670 rapidly induces NFIL3 expression in B cells and is required for promotion of IgE class switching
671 *in vivo* and *in vitro* (79). Furthermore, NFIL3 is induced by IL-4 in CD4^{+} T-cells via a STAT6-
672 dependent mechanism (80).
673
674 We identified the existence of two transcriptionally unique MMC9 populations; an inflammatory
675 MMC9 population that was enriched for transcripts involved in innate immune pathways and a
676 second MMC9 population that was enriched for transcripts involved in metabolic programming.

The inflammatory MMC9 population was enriched for Toll-like receptor signaling (*Ccl3, Ccl4, Il6, Nfkbia, Tollip*) and chemokine activity (*Ccl3, Ccl4*) suggesting a role for this cell population in innate immune activation and recruitment of inflammatory cells including monocytes and neutrophils. The metabolic MMC9 population was enriched for transcripts involved in the regulation of metabolic processes including pyruvate metabolism, oxidative phosphorylation and citric Acid (TCA) cycle (e.g. *Idh3b, Pdha1, Sdhc, Aldh3a2, Ndufs7, Uqcr11*) which suggests that this MMC9 population may utilize different metabolic processes for cellular function. Intriguingly, recent studies have demonstrated that mast cells may utilize metabolic reprogramming to shape immune responses in specific environments. IL-33 has been shown to stimulate glycolytic gene expression in mast cells and glycolytic ATP production is important for IL-33-induced mast cell activation (81). Furthermore, elevated glucose environment enhances FcεRI-dependent MC degranulation and LTC4 production (82). Given that mucosal barrier surfaces such as the gastrointestinal tract are metabolically distinct (reduced oxygen tension and nutrient levels) from other organs (83), metabolic reprogramming of MMC9 cells may be a response to the microenvironment and represent a mode by which these cells activate cellular function or preserve their maturation status at barrier sites. Interestingly, *in silco* analyses revealed that IL-4R-signaling seems to predominantly regulate metabolic processes within the MMC9 population. In particular, we show that IL-4 signaling-dysregulated transcripts were enriched in pathways focused around 2-oxoglutarate metabolic process, carbon and nitrogen metabolism and amino acid synthesis (e.g. *Chd9, Tbp, Mpg, Prmt5, Mrps12, Exosc4, Nt5c3b and Commd1*). The 2-oxoglutarate metabolic pathway serves as the convergence point of carbon and nitrogen metabolic pathways and regulates ATP production via glutamine-driven oxidative phosphorylation (84). The biological significance of IL-4Rα-regulation of metabolic programs in MMC9 cells in the context of food allergic reactions is not yet clear. The in vitro MMC9-L cells will provide an excellent system to begin to define the biological functions of MMC9 cells in vivo and the contribution of MMC9 populations to food allergy.

Herein we identified a mechanism whereby IL-4Ra signaling directly regulates MMC9 cell levels and subsequent induction of the dietary-antigen induced SI mastocytosis and food-induced anaphylaxis. The IL-4Rα-regulation of SI-MMC9 cells was associated with induction of IL-9, BATF and NFIL3, and in part dependent on BATF. Furthermore, we have identified two transcriptionally unique MMC9 populations that are distinguished by metabolic and inflammatory gene expression. Based upon these studies we conclude that IL-4Rα signaling regulates SI mastocytosis via control of MMC9 cells and suggests that blockade IL-4Rα-dependent

pathways would be effective in abrogating MC function and IgE-mediated food allergic response.

References:

1. Sampson HA. Update on food allergy. J Allergy Clin Immunol. 2004;113(5):805-19.
2. Gupta RS, Springston EE, Warrier MR, Smith B, Kumar R, Pongracic J, et al. The prevalence, severity, and distribution of childhood food allergy in the United States. Pediatrics. 2011;128(1):e9-17.
3. Branum AM, Lukacs SL. Food allergy among U.S. children: trends in prevalence and hospitalizations. NCHS data brief. 2008(10):1-8.
4. Gupta RS, Warren CM, Smith BM, Jiang J, Blumenstock JA, Davis MM, et al. Prevalence and Severity of Food Allergies Among US Adults. JAMA network open. 2019;2(1):e185630.
5. Sicherer SH, Sampson HA. Food allergy. J Allergy Clin Immunol. 2010;125(2 Suppl 2):S116-25.
6. Investigators PGoC, Vickery BP, Vereda A, Casale TB, Beyer K, du Toit G, et al. AR101 Oral Immunotherapy for Peanut Allergy. N Engl J Med. 2018;379(21):1991-2001.
7. Johnston LK, Chien KB, Bryce PJ. The immunology of food allergy. Journal of immunology (Baltimore, Md : 1950). 2014;192(6):2529-34.
8. Brandt EB, Strait RT, Hershko D, Wang Q, Muntel EE, Scribner TA, et al. Mast cells are required for experimental oral allergen-induced diarrhea. J Clin Invest. 2003;112(11):1666-77.
9. Kanagaratham C, Sallis BF, Fiebiger E. Experimental Models for Studying Food Allergy. Cellular and molecular gastroenterology and hepatology. 2018;6(3):356-69.e1.
10. Lee JB, Chen CY, Liu B, Mugge L, Angkasekwinai P, Facchinetti V, et al. IL-25 and CD4(+) TH2 cells enhance type 2 innate lymphoid cell-derived IL-13 production, which promotes IgE-mediated experimental food allergy. J Allergy Clin Immunol. 2016;137(4):1216-25.e5.
11. Paul WE, Zhu J. How are T(H)2-type immune responses initiated and amplified? Nat Rev Immunol. 2010;10:225-35.
12. Swain SL, Weinberg AD, English M, Huston G. IL-4 directs the development of Th2-like helper effectors. J-Immunol. 1990;145(11):3796-806 issn: 0022-1767.
13. Seder R, Paul W, Davis M, Groth B. The presence of interleukin 4 during in vitro priming determines the lymphokine-producing potential of CD4+ T cells from T cell Recepotr transgenic mice. J Exp Med. 1992;176:1091-8.
14. Osterfeld H, Ahrens R, Strait R, Finkelman FD, Renauld JC, Hogan SP. Differential roles for the IL-9/IL-9 receptor alpha-chain pathway in systemic and oral antigen-induced anaphylaxis. J Allergy Clin Immunol. 2010;125(2):469-76 e2.

15. Ahrens R, Osterfeld H, Wu D, Chen CY, Arumugam M, Groschwitz K, et al. Intestinal mast cell levels control severity of oral antigen-induced anaphylaxis in mice. The American journal of pathology. 2012;180(4):1535-46.
16. Noah TK, Knoop KA, McDonald KG, Gustafsson JK, Waggoner L, Vanoni S, et al. IL-13-induced intestinal secretory epithelial cell antigen passages are required for IgE-mediated food-induced anaphylaxis. J Allergy Clin Immunol. 2019.
17. Finkelman FD. Anaphylaxis: lessons from mouse models. J Allergy Clin Immunol. 2007;120:506-15.
18. Shik D, Tomar S, Lee JB, Chen CY, Smith A, Wang YH. IL-9-producing cells in the development of IgE-mediated food allergy. Seminars in immunopathology. 2017;39(1):69-77.
19. Chen CY, Lee JB, Liu B, Ohta S, Wang PY, Kartashov A, et al. Induction of Interleukin-9-producing Mucosal Mast cells Promotes Susceptibility to IgE-mediated Experimental Food Allergy. Immunity. 2015;43(4):788-802.
20. Licona-Limon P, Henao-Mejia J, Temann AU, Gagliani N, Licona-Limon I, Ishigame H, et al. Th9 Cells Drive Host Immunity against Gastrointestinal Worm Infection. Immunity. 2013;39(4):744-57.
21. Bao K, Carr T, Wu J, Barclay W, Jin J, Ciofani M, et al. BATF Modulates the Th2 Locus Control Region and Regulates CD4+ T Cell Fate during Antihelminth Immunity. Journal of immunology (Baltimore, Md : 1950). 2016;197(11):4371-81.
22. Miller MM, Patel PS, Bao K, Danhorn T, O'Connor BP, Reinhardt RL. BATF acts as an essential regulator of IL-25-responsive migratory ILC2 cell fate and function. Sci Immunol. 2020;5(43).
23. Forbes EE, Groschwitz K, Abonia JP, Brandt EB, Cohen E, Blanchard C, et al. IL-9- and mast cell-mediated intestinal permeability predisposes to oral antigen hypersensitivity. J Exp Med. 2008;205(4):897-913.
24. Arumugam M, Ahrens R, Osterfeld H, Kottyan LC, Shang X, Maclennan JA, et al. Increased susceptibility of 129SvEvBrd mice to IgE-Mast cell mediated anaphylaxis. BMC immunology. 2011;12:14.
25. Kim D, Langmead B, Salzberg SL. HISAT: a fast spliced aligner with low memory requirements. Nat Methods. 2015;12(4):357-60.
26. Liao Y, Smyth GK, Shi W. featureCounts: an efficient general purpose program for assigning sequence reads to genomic features. Bioinformatics (Oxford, England). 2014;30(7):923-30.
27. Thomas PD, Campbell MJ, Kejariwal A, Mi H, Karlak B, Daverman R, et al. PANTHER: a library of protein families and subfamilies indexed by function. Genome Res. 2003;13(9):2129-41.
28. Kanehisa M. Toward understanding the origin and evolution of cellular organisms. Protein Sci. 2019;28(11):1947-51.
29. Chen EY, Tan CM, Kou Y, Duan Q, Wang Z, Meirelles GV, et al. Enrichr: interactive and collaborative HTML5 gene list enrichment analysis tool. BMC bioinformatics. 2013;14:128.
30. Kuleshov MV, Jones MR, Rouillard AD, Fernandez NF, Duan Q, Wang Z, et al. Enrichr: a comprehensive gene set enrichment analysis web server 2016 update. Nucleic acids research. 2016;44(W1):W90-7.
31. Su AI, Cooke MP, Ching KA, Hakak Y, Walker JR, Wiltshire T, et al. Large-scale analysis of the human and mouse transcriptomes. Proc Natl Acad Sci U S A. 2002;99(7):4465-70.
32. Su AI, Wiltshire T, Batalov S, Lapp H, Ching KA, Block D, et al. A gene atlas of the mouse and human protein-encoding transcriptomes. Proc Natl Acad Sci U S A. 2004;101(16):6062-7.
33. Wu C, Macleod I, Su AI. BioGPS and MyGene.info: organizing online, gene-centric information. Nucleic acids research. 2013;41(Database issue):D561-5.
34. Szklarczyk D, Gable AL, Lyon D, Junge A, Wyder S, Huerta-Cepas J, et al. STRING v11: protein-protein association networks with increased coverage, supporting functional discovery in genome-wide experimental datasets. Nucleic acids research. 2019;47(D1):D607-d13.

Journal Pre-proof

35. Huang DW, Sherman BT, Tan Q, Collins JR, Alvord WG, Roayaei J, et al. The DAVID Gene Functional Classification Tool: a novel biological module-centric algorithm to functionally analyze large gene lists. Genome biology. 2007;8(9):R183.

36. Huang DW, Sherman BT, Tan Q, Kir J, Liu D, Bryant D, et al. DAVID Bioinformatics Resources: expanded annotation database and novel algorithms to better extract biology from large gene lists. Nucleic acids research. 2007;35(Web Server issue):W169-75.

37. Mi H, Muruganujan A, Ebert D, Huang X, Thomas PD. PANTHER version 14: more genomes, a new PANTHER GO-slim and improvements in enrichment analysis tools. Nucleic acids research. 2019;47(D1):D419-d26.

38. Mi H, Thomas P. PANTHER pathway: an ontology-based pathway database coupled with data analysis tools. Methods in molecular biology (Clifton, NJ). 2009;563:123-40.

39. McInnes L, Healy J, Melville J. Umap: Uniform manifold approximation and projection for dimension reduction. arXiv preprint arXiv:180203426. 2018.

40. Shannon P, Markiel A, Ozier O, Baliga NS, Wang JT, Ramage D, et al. Cytoscape: a software environment for integrated models of biomolecular interaction networks. Genome Res. 2003;13(11):2498-504.

41. Tachdjian R, Al Khatib S, Schwinglshackl A, Kim HS, Chen A, Blasioli J, et al. In vivo regulation of the allergic response by the IL-4 receptor alpha chain immunoreceptor tyrosine-based inhibitory motif. J Allergy Clin Immunol. 2010;125(5):1128-36 e8.

42. Noben-Trauth N, Shultz LD, Brombacher F, Urban JF, Jr., Gu H, Paul WE. An interleukin 4 (IL-4)-independent pathway for CD4+ T cell IL-4 production is revealed in IL-4 receptor-deficient mice. Proc Natl Acad Sci U S A. 1997;94(20):10838-43.

43. Dwyer DF, Barrett NA, Austen KF. Expression profiling of constitutive mast cells reveals a unique identity within the immune system. Nature immunology. 2016;17(7):878-87.

44. Kitamura Y. Heterogeneity of mast cells and phenotypic change between subpopulations. Annual review of immunology. 1989;7:59-76.

45. Lee F, Yokota T, Otsuka T, Meyerson P, Villaret D, Coffman R, et al. Isolation and characterization of a mouse interleukin cDNA clone that expresses B-cell stimulatory factor 1 activities and T-cell- and mast-cell-stimulating activities. Proc Natl Acad Sci U S A. 1986;83(7):2061-5.

46. Rennick D, Hunte B, Holland G, Thompson SL. Cofactors are essential for stem cell factor-dependent growth and maturation of mast cell progenitors: comparative effects of interleukin-3 (IL-3), IL-4, IL-10, and fibroblasts. Blood. 1995;85(1):57-65.

47. Smith CA, Rennick DM. Characterization of a murine lymphokine distinct from interleukin 2 and interleukin 3 (IL-3) possessing a T-cell growth factor activity and a mast-cell growth factor activity that synergizes with IL-3. Proc Natl Acad Sci U S A. 1986;83(6):1857-61.

48. Mosmann TR, Bond MW, Coffman RL, Ohara J, Paul WE. T-cell and mast cell lines respond to B-cell stimulatory factor 1. Proc Natl Acad Sci U S A. 1986;83(15):5654-8.

49. Hamaguchi Y, Kanakura Y, Fujita J, Takeda S, Nakano T, Tarui S, et al. Interleukin 4 as an essential factor for in vitro clonal growth of murine connective tissue-type mast cells. J Exp Med. 1987;165(1):268-73.

50. McLeod JJ, Baker B, Ryan JJ. Mast cell production and response to IL-4 and IL-13. Cytokine. 2015;75(1):57-61.

51. Bischoff SC, Sellge G. Mast cell hyperplasia: role of cytokines. Int Arch Allergy Immunol. 2002;127(2):118-22.

52. Coleman JW, Holliday MR, Kimber I, Zsebo KM, Galli SJ. Regulation of mouse peritoneal mast cell secretory function by stem cell factor, IL-3 or IL-4. Journal of immunology (Baltimore, Md : 1950). 1993;150(2):556-62.

53. Bischoff SC, Sellge G, Lorentz A, Sebald W, Raab R, Manns MP. IL-4 enhances proliferation and mediator release in mature human mast cells. Proc Natl Acad Sci USA. 1999;96:8080-5.
54. Toru H, Kinashi T, Ra C, Nonoyama S, Yata J, Nakahata T. Interleukin-4 induces homotypic aggregation of human mast cells by promoting LFA-1/ICAM-1 adhesion molecules. Blood. 1997;89(9):3296-302.
55. Valent P, Bevec D, Maurer D, Besemer J, Di Padova F, Butterfield JH, et al. Interleukin 4 promotes expression of mast cell ICAM-1 antigen. Proc Natl Acad Sci U S A. 1991;88(8):3339-42.
56. Ryan JJ, DeSimone S, Klisch G, Shelburne C, McReynolds LJ, Han K, et al. IL-4 inhibits mouse mast cell Fc epsilonRI expression through a STAT6-dependent mechanism. Journal of immunology (Baltimore, Md : 1950). 1998;161(12):6915-23.
57. Eklund KK, Ghildyal N, Austen KF, Stevens RL. Induction by IL-9 and suppression by IL-3 and IL-4 of the levels of chromosome 14-derived transcripts that encode late-expressed mouse mast cell proteases. Journal of immunology (Baltimore, Md : 1950). 1993;151(8):4266-73.
58. Matsuzawa S, Sakashita K, Kinoshita T, Ito S, Yamashita T, Koike K. IL-9 enhances the growth of human mast cell progenitors under stimulation with stem cell factor. Journal of immunology (Baltimore, Md : 1950). 2003;170(7):3461-7.
59. Burton OT, Darling AR, Zhou JS, Noval-Rivas M, Jones TG, Gurish MF, et al. Direct effects of IL-4 on mast cells drive their intestinal expansion and increase susceptibility to anaphylaxis in a murine model of food allergy. Mucosal immunology. 2012.
60. Arinobu Y, Iwasaki H, Gurish MF, Mizuno S, Shigematsu H, Ozawa H, et al. Developmental checkpoints of the basophil/mast cell lineages in adult murine hematopoiesis. Proceedings of the National Academy of Sciences of the United States of America. 2005;102(50):18105-10.
61. Hallgren J, Gurish MF. Mast cell progenitor trafficking and maturation. Advances in experimental medicine and biology. 2011;716:14-28.
62. Gurish MF, Boyce JA. Mast cells: ontogeny, homing, and recruitment of a unique innate effector cell. J Allergy Clin Immunol. 2006;117(6):1285-91.
63. Bankova LG, Dwyer DF, Liu AY, Austen KF, Gurish MF. Maturation of mast cell progenitors to mucosal mast cells during allergic pulmonary inflammation in mice. Mucosal immunology. 2015;8(3):596-606.
64. Gurish MF, Tao H, Abonia JP, Arya A, Friend DS, Parker CM, et al. Intestinal Mast Cell Progenitors Require CD49dbeta7 (alpha4beta7 Integrin) for Tissue-specific Homing. J Exp Med. 2001;194(9):1243-52.
65. Abonia JP, Austen KF, Rollins BJ, Joshi SK, Flavell RA, Kuziel WA, et al. Constitutive homing of mast cell progenitors to the intestine depends on autologous expression of the chemokine receptor CXCR2. Blood. 2005;105(11):4308-13.
66. Blom L, Poulsen BC, Jensen BM, Hansen A, Poulsen LK. IL-33 induces IL-9 production in human CD4+ T cells and basophils. PLoS One. 2011;6(7):e21695.
67. Vasanthakumar A, Moro K, Xin A, Liao Y, Gloury R, Kawamoto S, et al. The transcriptional regulators IRF4, BATF and IL-33 orchestrate development and maintenance of adipose tissue-resident regulatory T cells. Nature immunology. 2015;16(3):276-85.
68. Jabeen R, Goswami R, Awe O, Kulkarni A, Nguyen ET, Attenasio A, et al. Th9 cell development requires a BATF-regulated transcriptional network. J Clin Invest. 2013;123(11):4641-53.
69. Tsuda M, Hamade H, Thomas LS, Salumbides BC, Potdar AA, Wong MH, et al. A role for BATF3 in TH9 differentiation and T-cell-driven mucosal pathologies. Mucosal immunology. 2019;12(3):644-55.
70. Abdul Qayum A, Koh B, Martin RK, Kenworthy BT, Kharwadkar R, Fu Y, et al. The Il9 CNS-25 Regulatory Element Controls Mast Cell and Basophil IL-9 Production. Journal of immunology (Baltimore, Md : 1950). 2019;203(5):1111-21.
71. Fu Y, Koh B, Kuwahara M, Ulrich BJ, Kharwadkar R, Yamashita M, et al. BATF-Interacting Proteins Dictate Specificity in Th Subset Activity. Journal of immunology (Baltimore, Md : 1950). 2019.

Journal Pre-proof

72. Kuwahara M, Ise W, Ochi M, Suzuki J, Kometani K, Maruyama S, et al. Bach2-Batf interactions control Th2-type immune response by regulating the IL-4 amplification loop. Nature communications. 2016;7:12596.
73. Lee WH, Jang SW, Kim HS, Kim SH, Heo JI, Kim GE, et al. BATF3 is sufficient for the induction of Il9 expression and can compensate for BATF during Th9 cell differentiation. Experimental & molecular medicine. 2019;51(11):1-12.
74. Tussiwand R, Lee WL, Murphy TL, Mashayekhi M, Kc W, Albring JC, et al. Compensatory dendritic cell development mediated by BATF-IRF interactions. Nature. 2012;490(7421):502-7.
75. Ikushima S, Inukai T, Inaba T, Nimer SD, Cleveland JL, Look AT. Pivotal role for the NFIL3/E4BP4 transcription factor in interleukin 3-mediated survival of pro-B lymphocytes. Proc Natl Acad Sci U S A. 1997;94(6):2609-14.
76. Zhang W, Zhang J, Kornuc M, Kwan K, Frank R, Nimer SD. Molecular cloning and characterization of NF-IL3A, a transcriptional activator of the human interleukin-3 promoter. Molecular and cellular biology. 1995;15(11):6055-63.
77. Seillet C, Rankin LC, Groom JR, Mielke LA, Tellier J, Chopin M, et al. Nfil3 is required for the development of all innate lymphoid cell subsets. J Exp Med. 2014;211(9):1733-40.
78. Kashiwada M, Cassel SL, Colgan JD, Rothman PB. NFIL3/E4BP4 controls type 2 T helper cell cytokine expression. The EMBO journal. 2011;30(10):2071-82.
79. Kashiwada M, Levy DM, McKeag L, Murray K, Schroder AJ, Canfield SM, et al. IL-4-induced transcription factor NFIL3/E4BP4 controls IgE class switching. Proc Natl Acad Sci U S A. 2010;107(2):821-6.
80. Chen Z, Lund R, Aittokallio T, Kosonen M, Nevalainen O, Lahesmaa R. Identification of novel IL-4/Stat6-regulated genes in T lymphocytes. Journal of immunology (Baltimore, Md : 1950). 2003;171(7):3627-35.
81. Caslin HL, Taruselli MT, Haque T, Pondicherry N, Baldwin EA, Barnstein BO, et al. Inhibiting Glycolysis and ATP Production Attenuates IL-33-Mediated Mast Cell Function and Peritonitis. Front Immunol. 2018;9:3026.
82. Kitahata Y, Nunomura S, Terui T, Ra C. Prolonged culture of mast cells with high-glucose medium enhances the Fc epsilon RI-mediated degranulation response and leukotriene C4 production. Int Arch Allergy Immunol. 2010;152 Suppl 1:22-31.
83. Glover LE, Lee JS, Colgan SP. Oxygen metabolism and barrier regulation in the intestinal mucosa. J Clin Invest. 2016;126(10):3680-8.
84. Huergo LF, Dixon R. The Emergence of 2-Oxoglutarate as a Master Regulator Metabolite. Microbiol Mol Biol Rev. 2015;79(4):419-35.

Journal Pre-proof

933

934

935

936

937

938

939

940

941

942

Journal Pre-proof

943 **Figure legends**

944

945 **Figure 1: IL-4 signaling amplifies MMC9, CD4$^+$ Th2 cell and ILC2 frequency, and**
946 **increases severity and susceptibility of food-induced anaphylaxis.** (A)
947 Representative dotplots of MMC9s, CD4$^+$ Th2 cells and ILC2s, (B) IL-9 expression
948 within MMC9s, (C) frequencies and (D) absolute numbers of MMC9s, (E, F) frequencies
949 of CD4$^+$ Th2 cells and ILC2s, within SI-LP SSC^{lo} cells. (G) Representative
950 photomicrographs and (H) frequency of CAE$^+$ mast cells in the jejunum, (I) Diarrhea
951 incidence, (J) maximum body temperature change, (K) Hemocentration (%), (L) serum
952 MCPT-1 levels in OVA-sensitized WT, *Il4ra*^{Y709F} and *Il4ra*$^{-/-}$ mice. (A-E) Dotplots and
953 frequencies for MMC9s are pregated on Lin$^-$ CD3$^-$ CD4$^-$ IL-17RB- cells; for CD4$^+$ Th2
954 cells are pregated on Lin$^-$ CD3$^+$ CD4$^+$; and for ILC2s are pregated on Lin$^-$ CD3$^-$ CD4$^-$
955 cells. (B) Black line shows IL-9 expression compared to FMO control in grey, both
956 pregated on MMC9s. (C-F) Individual symbols represent one mouse; dash indicates
957 mean. (G) magnification X 20; insert X 40. (I-L) Data are presented as mean ± SEM;
958 n=12 - 20 mice per group, pooled from 3 - 4 independent experiments. (A-L) All
959 analyses show data for OVA-sensitized mice following the seventh oral
960 challenge.Statistical significance is * $p \leq 0.05$, ** $p \leq 0.01$, and **** $p < 0.0005$.
961 **Figure 2: IL-4 signaling intrinsically regulates SI-LP MMC9 development and**
962 **allergic outcomes in mice.** (A) Representative contour plots and (B, top row)
963 frequencies and absolute numbers of SI-LP MMC9s, (B, bottom row) frequencies of
964 CD4$^+$Th2 and ILC2 cells within the SI-LP SSC^{low} cells. (C) Diarrhea incidence, (D)
965 serum levels of MCPT-1, (E) CAE+ mast cell numbers in the jejunum, (F) serum OVA-
966 specific IgE levels and (G) *Il9* mRNA and secreted protein levels from WT or *Il4ra*^{Y709F}
967 or *Il4ra*$^{-/-}$ MMC9 cells purified from SI-LP. (A, B) Contour plots for frequencies of
968 MMC9s, CD4$^+$ Th2 cells and ILC2s are gated similar to Figure 1A-D. (B-F) individual
969 symbols represent one mouse; dash indicates mean ± SEM; n = 12 - 24 mice per group,
970 pooled from 3 - 4 independent experiments. (C) The fraction represents the number of
971 mice with diarrhea as part of the total number of mice. (G) Individual symbols represent
972 one mouse; dash indicates mean ± SEM; n =4 mice per group. (A-G) Analyses shows
973 data from OVA-sensitized WT mice that received WT or *Il4ra*^{Y709F} or *Il4ra*$^{-/-}$ BM,

following seventh oral challenge. Statistical significance is * $p \leq .005$, ** $p \leq 0.01$, and **** $p < 0.0005$. ns, not significant.

Figure 3: IL-4 signaling intrinsically regulates MMC9 gene expression profile. (A) Venn diagram describing altered gene expression within *Il4ra*^{Y709F} (blue) or *Il4ra*$^{-/-}$ (yellow) MMC9s, as compared to WT MMC9s identified by RNA-seq analyses from sorted SI-LP-MMC9s. (B) Heat Map showing fold change in expression of the 410 reciprocally regulated genes and (C) Fold changes in the expression of the top 19 reciprocally regulated genes increased in *Il4ra*^{Y709F}-MMC9s (red) and top 19 reciprocally regulated genes increased in *Il4ra*$^{-/-}$- MMC9s (blue), as compared to WT MMC9s. (D) Expression of *Il9*, *Nfil3*, *Batf* genes in WT, *Il4ra*^{Y709F}- and *Il4ra*$^{-/-}$ MMC9s, (E) Spearman correlation analyses of *Il9*/*Batf* and (F) *Il9*/*Nfil3* mRNA expression by RNA-seq for flow sorted SI-MMC9s, SI-ILC2s, SI Th2 cells, BMMCs, peritoneal mast cells, mast cell progenitors (MCps), CD4^{+} non Th2 cells, CD8^{+} T cells, B cells and eosinophils as described (19). (G) Venn diagram demonstrating differentially expressed genes in MMC9 cells (GSE72921) (19) and sort purified Lin-GFP^{hi} IL-17RB^{-} c-Kit^{+} ST2^{+} β7integrin^{low} WT-origin SI-MMC9 cells of food allergic recipient mice that received WT BM, to identify a common 3491 MMC9 transcriptome. (H) Graphical representation of the Top 10 enriched pathways of the MMC9 transcriptome using DAVID analysis.

Figure 4: scRNA-seq analyses of SI MMC9 cells. (A) Heat map showing Prioritization mapping (average RPKM values) and (B) String protein-protein interaction network analysis of the top 50 gene transcripts within 75 single flow sorted SI- Lin^{-}GFP^{hi} IL-17RB^{-} c-Kit^{+} ST2^{+} β7integrin^{low} cells from WT mice food allergic mice. (C). UMAP based- gene expression dimensional reduction and clustering of n = 71 MMC9 cells into three distinct clusters (Cluster 0 (n = 30 cells) (metabolic), 1 (n = 24 cells) (inflammatory) and (n = 17 cells) 2 (other)). (D) Heat map of the top 30 transcripts (average RPKM values) enriched in MMC9 Clusters (Metabolic = total 370 genes; Inflammatory = 19 genes and other n = 5 genes). (B) Network nodes represent proteins encoded by the genes. Functional partner predictions are based on available experimental data, databases, text mining, and homology.

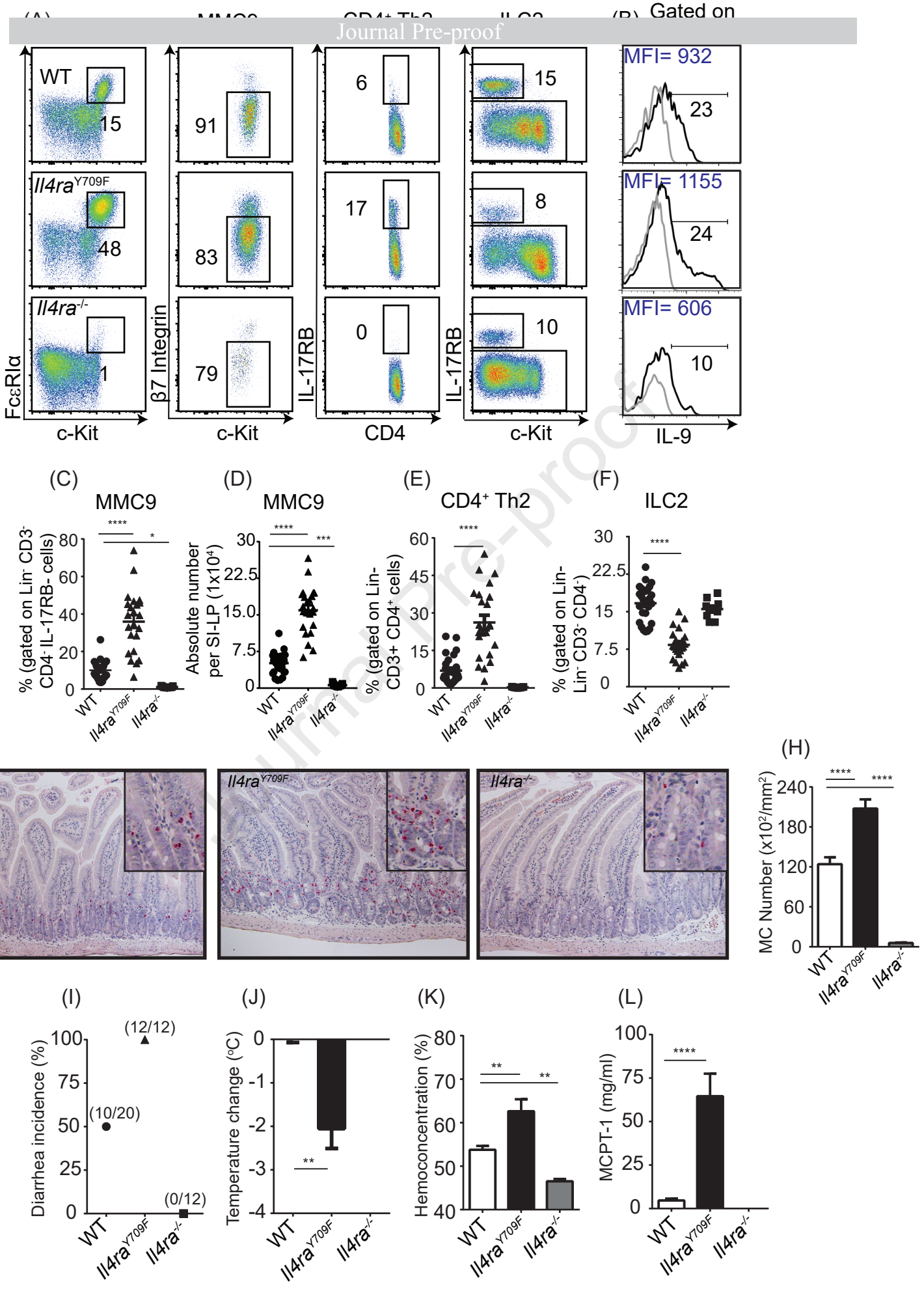
Figure 5: Gene identification and pathway Network Analyses of the IL-4R responsive transcripts in the metabolic MMC9 cluster. Gene-pathway network

analysis of the 100 IL-4R responsive genes enriched in the metabolic MMC9 cluster. IL-4R DEGs identified from bulk culture RNA-seq WT, *Il4ra*^{Y709F} or *Il4ra*$^{-/-}$ MMC9 analyses were mapped over 3 different clusters (metabolic, inflammatory and others) and significant enrichment was identified with the Metabolic Cluster. Up arrows indicate upregulated DEGs and down arrows show down regulated DEGs (when compared with WT MMC9). Color code of arrow indicates expression pattern of DEG. Green indicates *Il4ra*^{Y709F} DEGs only; Red indicates *Il4ra*$^{-/-}$ DEGs only; Magenta indicates DEGs upregulated in *Il4ra*^{Y709F} and downregulated / no changed in *Il4ra*$^{-/-}$. Olive indicates DEGs upregulated in *Il4ra*$^{-/-}$ and downregulated / no changed in *Il4ra*^{Y709F}. Light purple indicates DEGs upregulated in *Il4ra*$^{-/-}$ and *Il4ra*^{Y709F}. Lines indicate connections between genes and DAVID and String enriched pathways.

Figure 6: IL-4 signaling regulates IL-9 expression in bone marrow-derived MMC9-L cells. (A) Outline of the cytokine stimulation time course for bone marrow-derived MMC9-like protocol, as described in Methods. (B) Representative contour plots and gating strategy to identify MMC9-like cells from IL-9-GFP mice when cultured in mSCF, mIL-3 (media) with (top) or without mIL-4 (bottom) for 4 days and then stimulated with mIL-33 for 24h, after an initial culture in mSCF and mIL-3 for 6 days. (C) Graphical representation of frequency of IL-9-GFP^{+} MMC9-L cells and mature IL9^{+} mast cells within (Lin^{-} CD27^{-}) c-Kit^{+} FcεRIα^{-} or c-Kit^{+} FcεRIα^{+} respectively, as shown in (B). (D) Representative contour plots and gating strategy to identify MMC9-like cells from WT and *Batf*$^{-/-}$ mice, following a MMC9-L-derivation protocol described above, with IL-9^{+} cells identified by intracellular staining for IL-9. (E) Graphical representation of IL-9^{+} MMC9-L cells within (Lin^{-}) c-Kit^{+} FcεRIα^{-} cells as shown in (D). Data shown represents mean ± SEM, n= 4 - 5 mice each group. Statistical significance is * $p \leq 0.005$, ** $p \leq 0.01$, and **** $p < 0.0005$

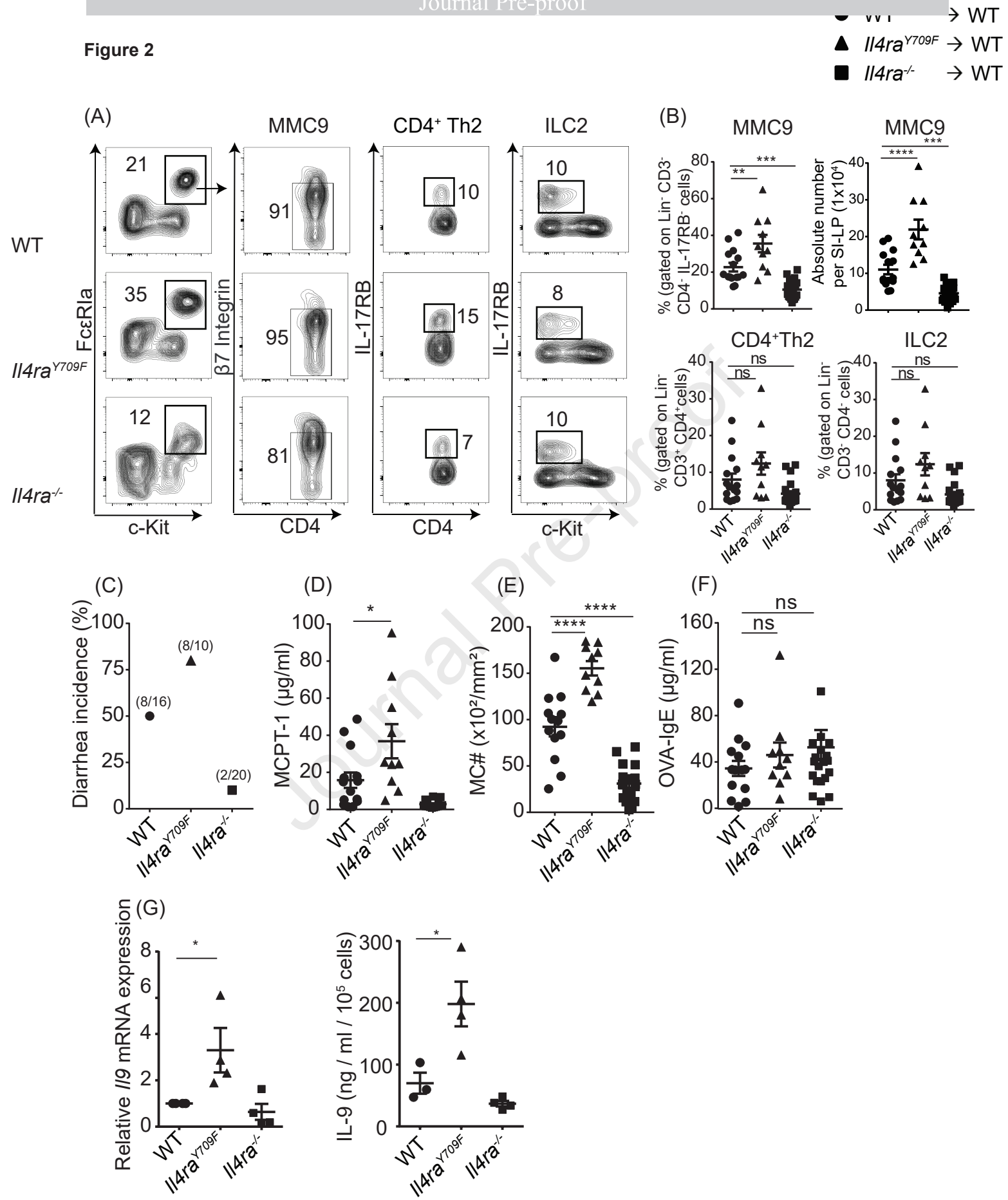
Figure1

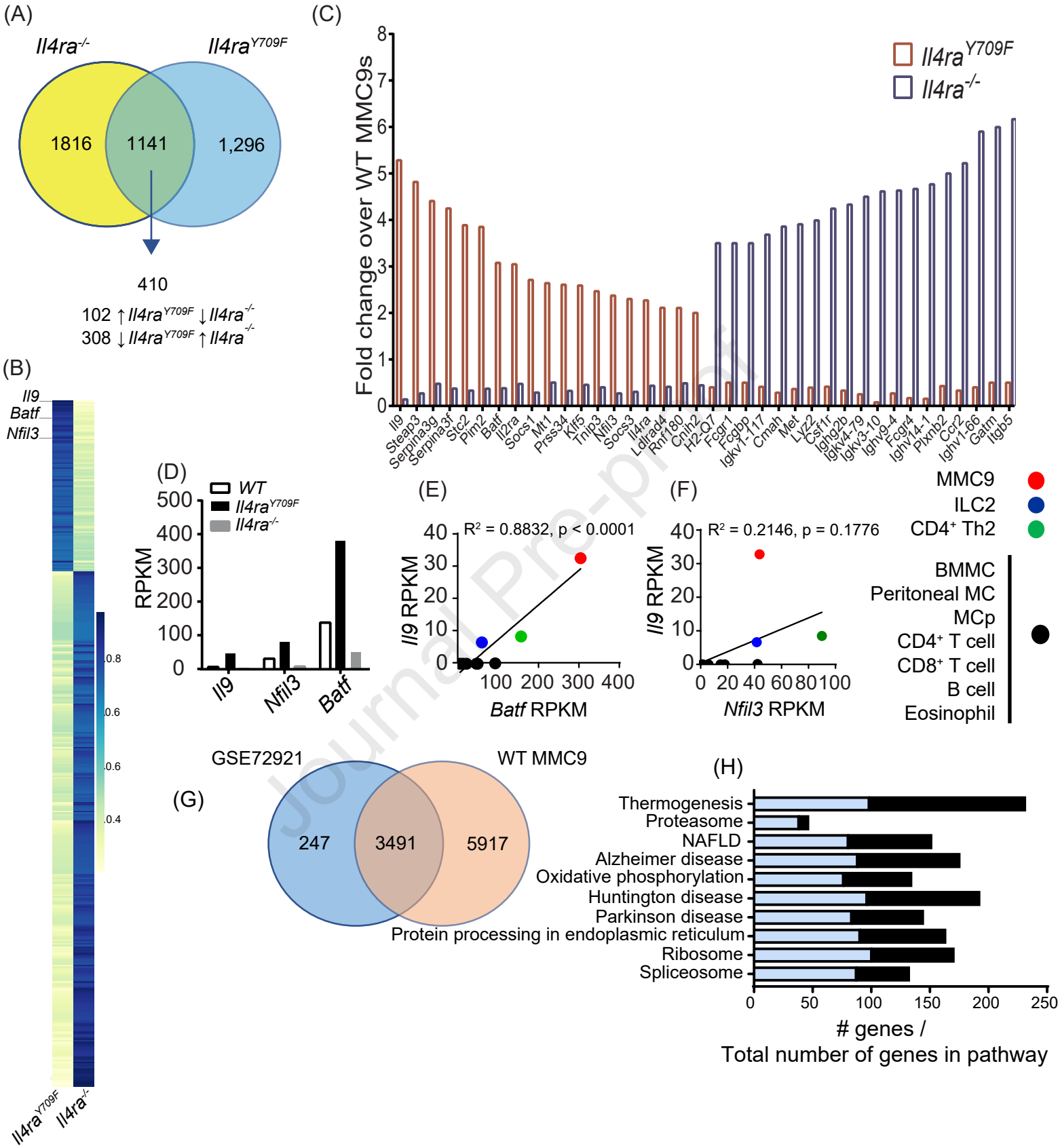
Journal Pre-proof



Journal Pre-proof

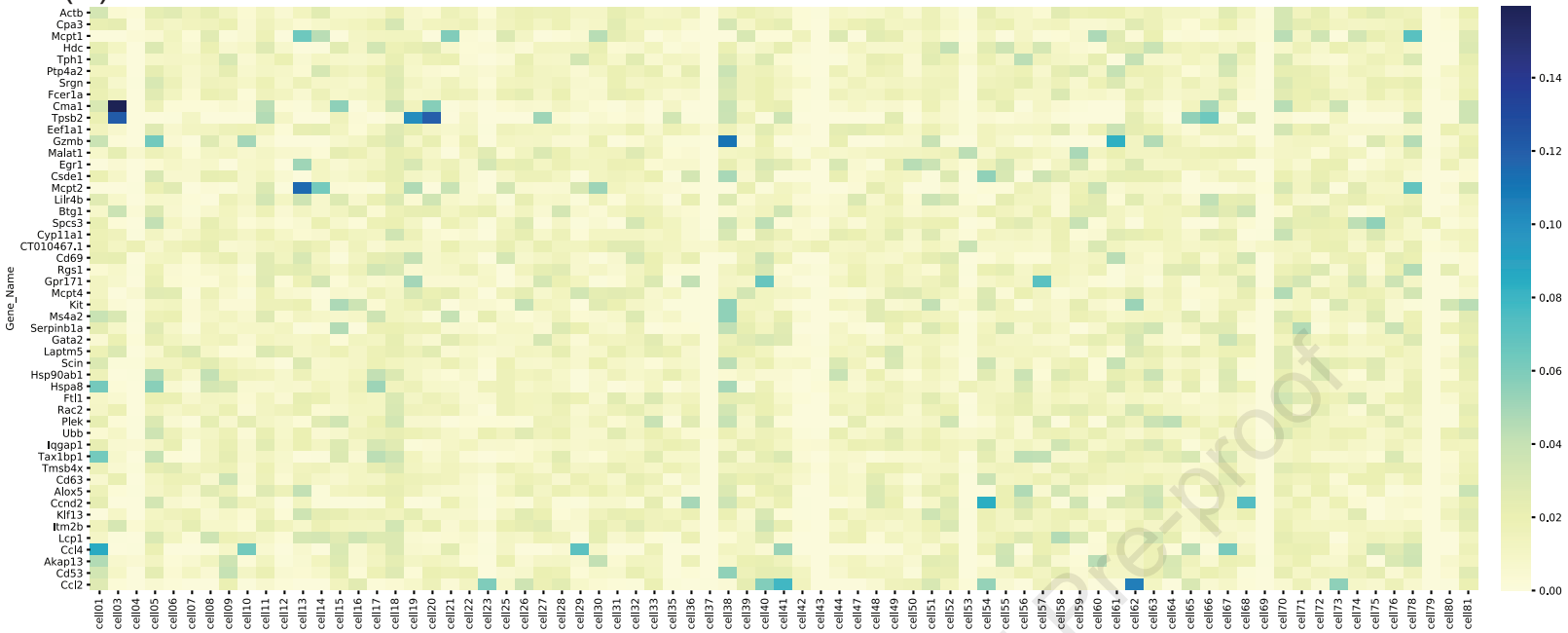
Figure 2

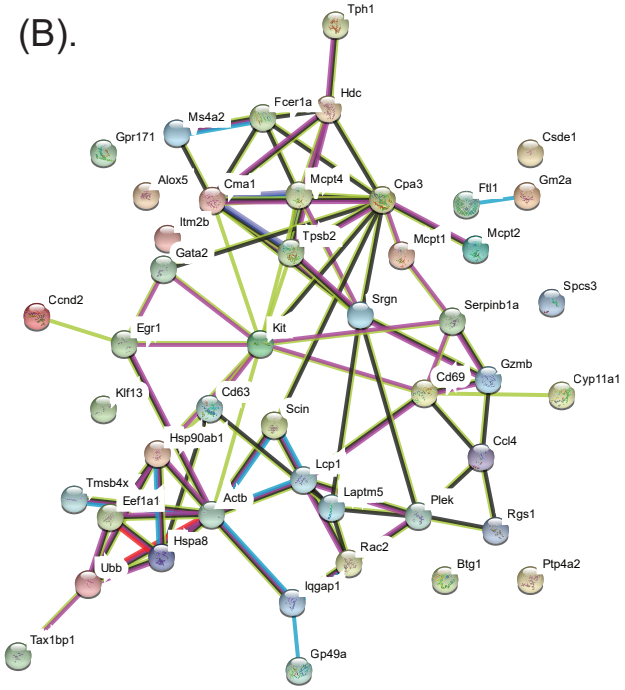


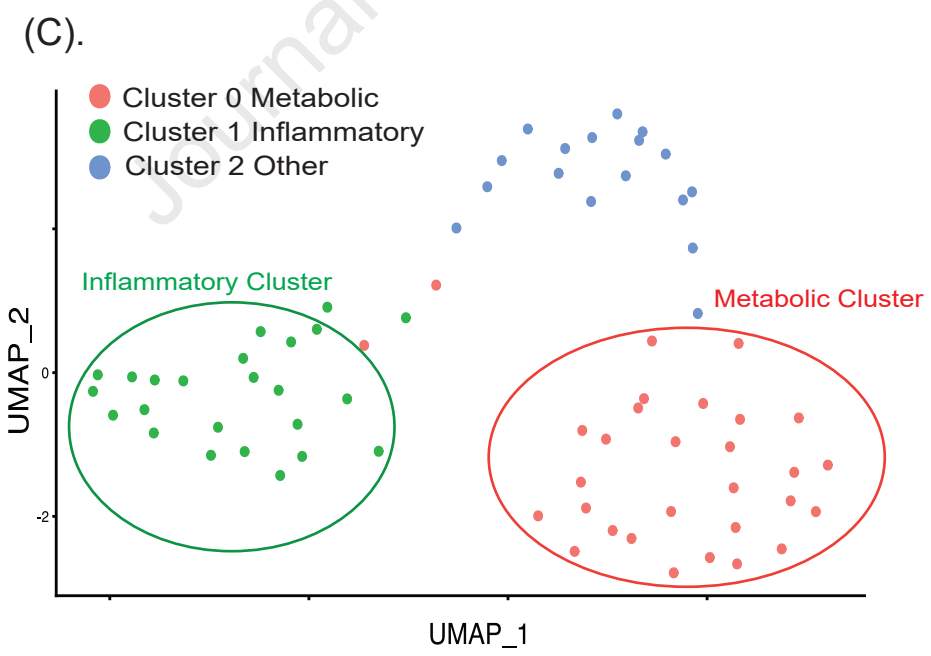

(A)
Il4ra-/-
Il4raY709F
1816
1141
1,296
410
102 ↑Il4raY709F ↓Il4ra-/-
308 ↓Il4raY709F ↑Il4ra-/-
(B)
Il9
Batf
Nfil3
Il4raY709F
Il4ra-/-
(C)
Fold change over WT MMC9s
Il4raY709F
Il4ra-/-
Il9 Steap3 Serpina3g Serpina3f Stc2 Pim2 Batf Il2ra Socs1 Mt1 Prss34 Klf5 Tnip3 Nfil3 Socs3 Il4ra Ldlrad4 Rnf180 Cnih2 H2-Q7 Fcgr1 Fcgbp Igkv1-117 Cmah Met Lyz2 Csf1r Ighg2b Igkv4-79 Igkv3-10 Ighv9-4 Fcgr4 Ighv14-1 Plxnb2 Ccr2 Ighv1-66 Gatm Itgb5
(D)
WT
Il4raY709F
Il4ra-/-
RPKM
Il9
Nfil3
Batf
(E)
R² = 0.8832, p < 0.0001
Il9 RPKM
Batf RPKM
(F)
R² = 0.2146, p = 0.1776
Il9 RPKM
Nfil3 RPKM
MMC9
ILC2
CD4⁺ Th2
BMMC
Peritoneal MC
MCp
CD4⁺ T cell
CD8⁺ T cell
B cell
Eosinophil
(G)
GSE72921
WT MMC9
247
3491
5917
(H)
Thermogenesis
Proteasome
NAFLD
Alzheimer disease
Oxidative phosphorylation
Huntington disease
Parkinson disease
Protein processing in endoplasmic reticulum
Ribosome
Spliceosome
genes /
Total number of genes in pathway

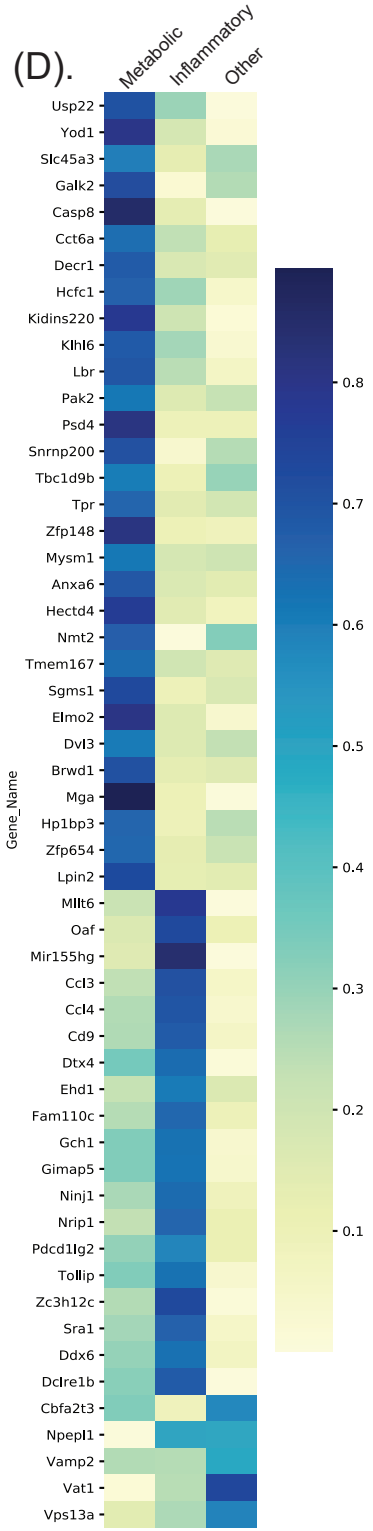
Journal Pre-proof

Figure 4



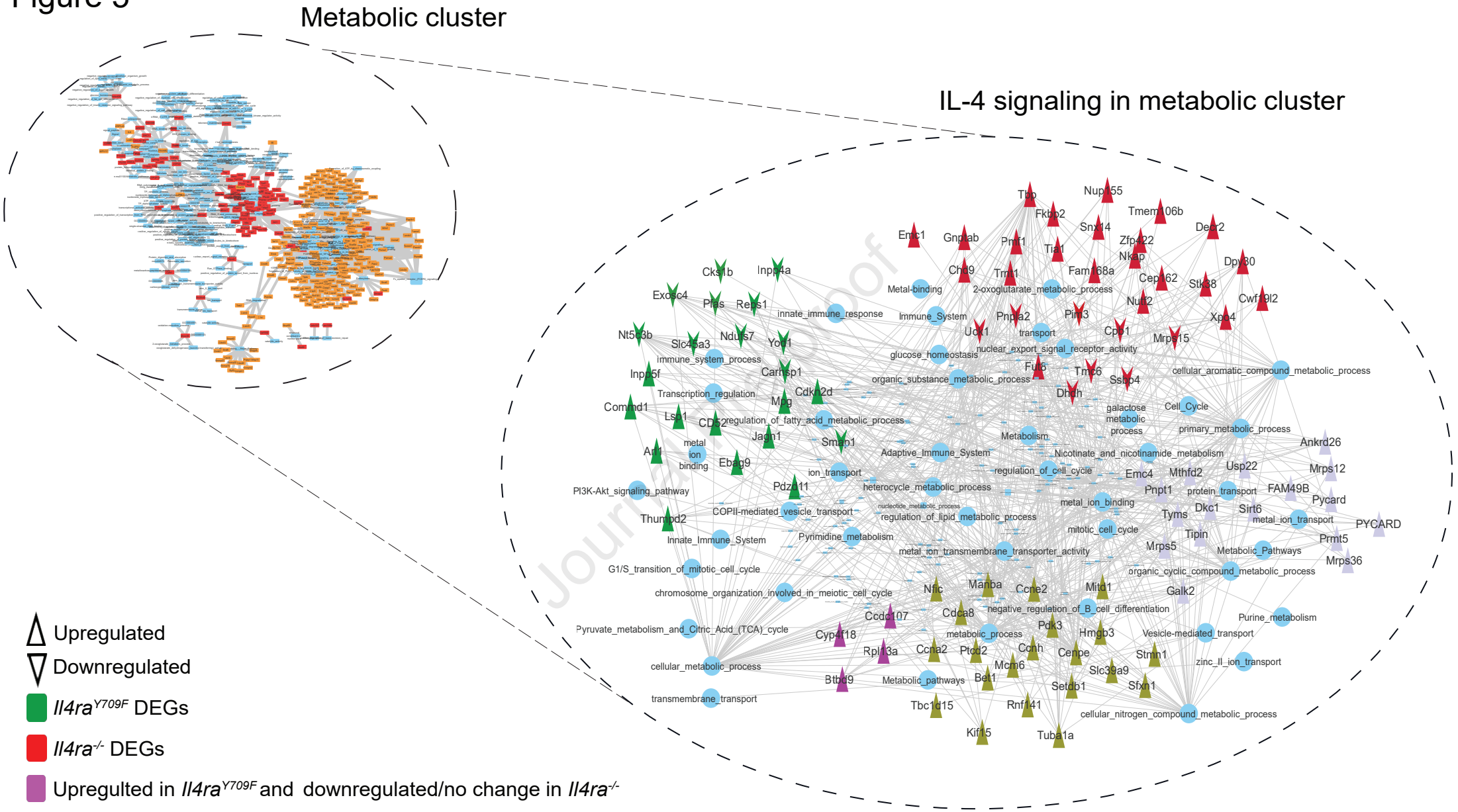






Journal Pre-proof

Figure 5



Journal Pre-proof

Figure 6

